# Analysis of aromatic carboxylic acid and calcium salt couples with gas chromatography-mass spectrometry: Implications and comparison with in situ measurements at Mars' surface

Ophélie Mcintosh, Caroline Freissinet, A. Buch, J.M.T. Lewis, Maëva Millan, A.J. Williams, T. Fornaro, J.L. Eigenbrode, J. Brucato, Cyril Szopa

Icarus 413 (2024) 116015

Contents lists available at ScienceDirect

Icarus

journal homepage: www.elsevier.com/locate/icarus

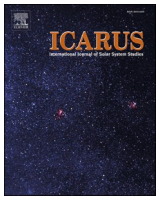

# Analysis of aromatic carboxylic acid and calcium salt couples with gas chromatography-mass spectrometry: Implications and comparison with *in situ* measurements at Mars' surface

O. McIntosh [a,b,*], C. Freissinet [a], A. Buch [c], J.M.T. Lewis [d,e,f], M. Millan [a], A.J. Williams [g], T. Fornaro [b], J.L. Eigenbrode [d], J. Brucato [b], C. Szopa [a]

[a] LATMOS/IPSL, UVSQ University Paris-Saclay, Sorbonne University, CNRS, 11 Bd d'Alembert, 78280 Guyancourt, France
[b] INAF- Astrophysical Observatory of Arcetri, L.go E. Fermi 5, 50125 Firenze, Italy
[c] Laboratoire Génie des Procédés et Matériaux, CentraleSupélec, University Paris-Saclay, 8-10 rue Joliot-Curie, 91190 Gif-sur-Yvette, France
[d] NASA Goddard Space Flight Center, Greenbelt, MD, USA
[e] Center for Research and Exploration in Space Science and Technology, NASA GSFC, Greenbelt, MD, USA
[f] Department of Physics and Astronomy, Howard University, Washington, DC, USA
[g] Department of Geological Sciences, University of Florida, Gainesville, FL 32611, USA

ARTICLE INFO

*Keywords:*
Aromatic organic salts
Gas chromatography-mass spectrometry
Pyrolysis,derivatization
Mars

ABSTRACT

Aromatic organic salts such as benzoates or phthalates may be widespread degradation products of organic molecules at the surface of Mars. The low volatility of these aromatic carboxylic salts could have compromised their detection through thermal extraction *in situ* analyses such as those performed by the Viking landers. However, over the years, analytical chemistry laboratories on board current and future Martian surface missions, such as the Sample Analysis at Mars (SAM) instrument suite on board the Curiosity rover and the Mars Organic Molecule Analyzer (MOMA) instrument of the Rosalind Franklin ExoMars rover, respectively, have evolved. These instruments have improved in efficiency to detect refractory and polar organic compounds, which could influence the detection of aromatic organic salts. To evaluate the capability of detecting aromatic organic salts on Mars with *in situ* instruments, we performed laboratory experiments under Viking, SAM, and MOMA-like Gas Chromatography-Mass Spectrometry (GC–MS) conditions with two carboxylic acid/salt couples: phthalic acid/calcium phthalate and benzoic acid/calcium benzoate. We studied the behavior and signatures of both molecular forms when using pyrolysis and derivatization experiments and the implications of these results in the search for organic molecules on Mars. This study showed that the Viking experiments could not have detected the presence of aromatic carboxylic salts in Martian samples because its maximum pyrolysis temperature was too low (500 °C). However, we showed that calcium benzoate and calcium phthalate, despite their refractory nature, could be identified indirectly through the detection of thermal and derivatized degradation products, both with SAM and MOMA. No conclusive proof of the presence of these aromatic organic salt species have been found in the SAM *in situ* data but given the right instrumental set-up they could be detected if present. The conclusions of this work raise essential questions on the detectability of refractory molecules, the analytical efficiency of flight instruments, and the interpretation of *in situ* data.

## 1. Introduction

The detection and identification of organic molecules on Mars are of primary importance to establish the existence of a possible ancient prebiotic chemistry or even past or present biological activity and is, therefore, a central goal for Mars exploration missions. A small diversity of organic molecules has been identified such as hydrocarbons, chloroorganics and sulfur-bearing compounds. (Eigenbrode et al., 2018; Freissinet et al., 2015; Millan et al., 2022; Szopa et al., 2020) despite the harsh environmental conditions present at the surface. Several factors can be involved in this low detection: (a) high doses of ionizing electromagnetic and particle radiation penetrating the thin Martian

* Corresponding author at: LATMOS/OVSQ, 11 boulevard d'Alembert, 78280 Guyancourt, France.
*E-mail address:* ophelie.mcintosh@latmos.ipsl.fr (O. McIntosh).

https://doi.org/10.1016/j.icarus.2024.116015
Received 15 May 2023; Received in revised form 31 January 2024; Accepted 23 February 2024
Available online 2 March 2024

atmosphere, leading to the destruction or transformation of surface organic compounds, (b) presence of strong oxidants on the soil, (c) technical biases of current flight-instruments such as high temperature pyrolysis or thermochemolysis which could lead to the thermal degradation of organic molecules and (d) insufficient instrument sensitivity. The harsh oxidative and radiative conditions of the Martian environment influence the fate of organic molecules present on its surface. Organic compounds, either endogenous to Mars or from exogenous sources such as meteorites, likely undergo oxidative processes due to the oxidants present in the Martian soil (*e.g.,* oxychlorines such as perchlorates, or hydrogen peroxide ($H_2O_2$)) (Glavin et al., 2013; Lasne et al., 2016). On Mars, these oxidation processes are also likely accelerated by the presence of iron mineral catalysts (Hassler et al., 2013). Moreover, the surface of Mars is exposed to ultraviolet radiation with wavelengths above 190 nm, which is efficiently absorbed by organic molecules producing photochemical reactions in very short timescales and it is sufficiently energetic to cleave water condensed on mineral surfaces producing free radicals and molecules ($H^+$, $OH^+$, $H_2O_2$) that can oxidize organic molecules (Fornaro et al., 2018). The formation of these radical species may transform organic macromolecules into carboxylic acids through Fenton chemistry (Benner et al., 2000; Oró and Holzer, 1979a, 1979b) or *via* the irradiation of semiconductor surfaces (possibly clay minerals) (Fox et al., 2019). In this study, we focused on two aromatic carboxylic acids: phthalic acid and benzoic acid. These molecules are thought to be abundant on the Martian surface as they are in stable intermediate oxidation states and can be formed from the oxidation of Polycyclic Aromatic Hydrocarbons (PAHs) or alkylbenzene compounds (Benner et al., 2000; Oró and Holzer, 1979a, 1979b). Moreover, benzoic acid has been detected with the Sample Analysis at Mars (SAM) instrumental suite on board the Curiosity rover (Millan et al., 2022; Williams et al., 2021), and is considered to be a potential precursor for the chlorinated aromatic organic molecules detected on Mars (Freissinet et al., 2020). Because benzene carboxylates are metastable, they would not be entirely oxidized into volatile molecules such as $CO_2$ or $O_2$, but instead, ionized by solar radiation to form organic salts (Benner et al., 2000; Kminek and Bada, 2006; Lasne et al., 2016; Pavlov et al., 2022). Benner et al. (2000) suggested that the low volatility of these salts could have compromised their *in situ* detection through thermal extraction analyses as performed by the Viking landers (Hakkinen et al., 2014). These assumptions are still relevant today as SAM and the Mars Organic Molecule Analyzer (MOMA) instrument of the Rosalind Franklin ExoMars rover, also perform pyrolysis experiments to analyze the molecular composition of the Martian surface. However, whereas the Viking experiments were set to perform flash pyrolysis to a maximum temperature of 500 °C, SAM and MOMA can reach temperatures above 800 °C, therefore widening the window of detectability for low volatility compounds or their thermal decomposition products. Moreover, SAM and MOMA have the capability to perform derivatization experiments which increases the volatility of refractory materials without thermal degradation of the parent molecule. A recent laboratory study by Lewis et al. (2021) examined the $CO_2$ and CO evolutions produced by the thermal decomposition of small aliphatic organic salts, which were then compared to data from SAM Evolved Gas Analysis (EGA) experiments. Numerous fits between laboratory and SAM data were observed, indicating that organic salts are compelling candidates for many SAM $CO_2$ and CO peaks but EGA data alone cannot conclusively identify organic salts.

To complement the Lewis et al. (2021) study and to investigate aromatic organic salts molecules through their direct or indirect detection on Mars, we performed laboratory tests using SAM and MOMA-like Gas Chromatography-Mass Spectrometry (GC–MS) analyses of two acid/salt couples: phthalic acid/calcium phthalate and benzoic acid/calcium benzoate.

The widespread availability of calcium on Mars makes it an element of high interest to form organic salt complexes. The calculated representative *in situ* mass fraction of calcium at different landing sites was evaluated between ~4.0 and 4.6% (Karunatillake et al., 2007). Geochemical analysis, from the ChemCam instrument onboard the Curiosity rover at Gale Crater, reported enhanced calcium associated to sulfur detection interpreted as Ca-sulfates (Nachon et al., 2017) disseminated in the bedrock at 30–50 wt% (Rapin et al., 2019). In Oxia Planum, the planned landing site of the Rosalind Franklin rover, calcium pyroxene signatures were detected from orbit with the Compact Reconnaissance Imaging Spectrometer for Mars (CRISM) aboard the Mars Reconnaissance Orbiter (MRO) (Seelos et al., 2014). Additionally, a Ca/K ratio $>$ 5 wt% was detected by the Viking X-ray fluorescence spectrometer (Toulmin III et al., 1976) as well as the elemental analysis of the Viking landing sites reporting a significant concentration of several elements like calcium in the Martian regolith (Clark et al., 1976). Finally, the possible presence of calcium chloride brines was also reported by Brass (1980) and Ca-perchlorates were detected at Gale Crater with SAM (Glavin et al., 2013; Ming et al., 2014).

If organic salts can be confirmed to be present on Mars, it would help better understand the transformation of organic matter under the harsh conditions of the Martian surface. Moreover, organic salts can originate from metabolic processes that can be preserved in the geological record (Jehlička and Edwards, 2008), making them primary targets for *in situ* molecular analyses.

## 2. Materials and methods

### 2.1. Studied analytes

This study was focused on two aromatic carboxylic acid species: phthalic acid and benzoic acid. The corresponding aromatic carboxylic salts were selected to be linked with calcium as the carboxylic acids could have reacted with the calcium present at the Martian surface.

Moreover, both calcium phthalate and calcium benzoate were available commercially and allowed consistency with the cation involved in the reaction pathway for both carboxylic acids.

All products were commercially sourced. The benzoic acid $C_6H_5COOH$ ($\geq$ 99.5%) and 1,2-benzenedioic acid (phthalic acid) ($C_6H_4$–1,2-$(CO_2H)_2$) ($\geq$ 99.5%) were purchased from Merck. The calcium benzoate trihydrate ($C_{14}H_{10}CaO_4$. $3H_2O$) was purchased from Unites States Pharmacopeia (USP) and calcium phthalate hydrate ($C_8H_4CaO_4.H_2O$) (98%) from Combi-Blocks.

### 2.2. Sample preparation

Organic molecules and salts would most likely be present as trace components (~ 100 ppbw) in Martian soil composed of amorphous and crystalline inorganic phases (Rampe et al., 2020). In order to simulate such conditions in our experiments, the carboxylic acid and calcium salts standards were dispersed in a chemically inert matrix of fused synthetic silica quartz (Schlten and Leinweber, 1993)(~44 μm grain size powder, supplied by Sigma-Aldrich). The fused silica was conditioned at 1000 °C for 24 h in an oven to remove any potential organic contamination. Each of the organic compounds studied were diluted in the silica in their solid form at 1:100 mixing ratios for the acid and 2.3:100 and 1.2:100 for calcium benzoate and calcium phthalate, respectively, in order to obtain the same molar abundance with the acids and their respective salts. The solid samples were ground to a powder and mixed in an organically-clean porcelain mortar and pestle which had been baked at 500 °C for two hours prior to sample preparation. To ensure a better homogenization of the powders, the samples were further mixed in a CryoMill Ball Mill (Retsch) (25 Hz for 10 min).

### 2.3. Instrumentation

The pyrolysis instrumental procedures were performed using a Frontier Laboratories 3030D multi-shot pyrolyzer (FrontierLab) mounted on the split/spitless injector of a gas chromatograph Trace Ultra

coupled to an ISQ quadrupole mass spectrometer (both from Thermo-Scientific). The pyrolysis oven was in the carrier gas (Helium, purity >99,999%, Air Liquide) flow pathway (1.0 mL·min$^{-1}$), allowing all the gaseous species produced in the chamber to be instantaneously transferred to the injector. For the derivatization experiments, the derivatization reaction was performed offline and the subsequent injection was made directly through the gas chromatograph injector with a micro-volume liquid syringe.

### 2.4. Evolved Gas Analysis (EGA)

Prior to EGA analyses, the samples were deposited in a Frontier Lab stainless steel Eco-Cups pre-cleaned with ethanol (purity >95%, Merck) and heated red with a burner (about 1400 °C). 5 mg of the organic/silica mixture were then deposited in the cup and weighed with a microscale (Mettler Toledo) that was precise to 0.001 mg. The sample cup was then lowered into the pyrolysis oven.

The EGA experiments were conducted using an inert Ultra ALLOY-DTM metallic tube (2.5 m long; 0.15 mm internal diameter - Frontier Lab), connected on one end to the GC injector and on the other end to the MS with a deactivated fused silica transfer line (0.4 m long; 0.25 mm internal diameter). The short length of the tube minmized the duration of transfer of the gases from the injector to the mass spectrometer (~10 s), with a constant helium flow of 1 mL·min$^{-1}$. The tube was maintained at an isothermal temperature of 250 °C throughout the run to limit any condensation. The GC injector was set in a split mode with a 1:20 split ratio. The ion source and transfer line temperatures of the MS were both set at 300 °C, and ions produced by electron impacts (energy of 70 eV) were scanned between masse to charge ratios ($m/z$) of 10 to 400.

Among the Mars instruments relevant to this study, only SAM can perform EGA. For this reason, the samples were heated from 80 °C to 800 °C with a temperature ramp of 35 °C·min$^{-1}$ to mimic SAM EGA temperature conditions. The time scale given by the chromatographic analysis was converted into temperature scale for EGA by simply using the heating rate of the pyrolysis and the known time of transfer between the pyrolyzer and the MS.

Blank runs were performed between each sample analysis in order to ensure the absence of contamination from the previous experiment. When contamination was detected, the pyrolyzer-GC–MS chain was cleaned by heating the whole sample pathway at the maximum temperature. Each analysis was repeated twice to ensure repeatability.

### 2.5. Pyrolysis-GC–MS

The sample preparation procedure was identical to the one described above for the EGA experiments.

Three sets pyrolysis conditions were tested: Viking-like, MOMA-like, and SAM-like.

To simulate SAM experiments, the samples were slowly heated in the pyrolyzer furnace from 80 °C to 800 °C with a 35 °C·min$^{-1}$ ramp. The volatiles evolved from the sample throughout the entire duration of the ramp, *i.e.*, in about 22 min. To mimic the Injection Trap (IT) present ahead of three out of six SAM GC columns and utilized to preconcentrate the analytes and to increase the separation power of the chromatograph (Mahaffy et al., 2012), the gases were condensed at the GC column inlet during the whole pyrolysis phase using a cryogenic trap. The cryotrap used a liquid nitrogen cooling system (T ~ −180 °C) supplied by FrontierLab, which was directly coupled to the pyrolyzer control system. Once the pyrolysis was completed, the cryotrap was stopped. The condensates were quickly vaporized to flow through the chromatographic column for their separation with the GC and detection with the MS.

For the MOMA-like experiments, the fast temperature ramp (200 °C. min$^{-1}$) (Goesmann et al., 2017) which will be performed by the flight instrument present a non-linear heating profile, difficult to accurately simulate with our laboratory setup. Therefore, we performed experiments using flash pyrolysis where the samples were directly heated to the maximal temperature (800 °C) attainable by the MOMA instrument for a few minutes. In the flash heating mode, the chromatographic analysis started as soon as the sample was introduced into the pyrolizer; the gases were produced and transferred to the GC instantaneously.

Finally, the Viking-like experiments consisted in flash heating the samples (within seconds) to 500 °C, held for thirty seconds at this temperature.

For the chromatographic analyses, we used a Zebron 5MS Plus column with a 5% Phenyl-Arylene, 95% Dimethylpolysiloxane stationary phase (30 m long; 0.25 mm internal diameter, 0.25 µm stationary phase thickness) (Phenomenex®) equipped with a 5-m long integrated guard line to protect the analytical column from contamination and fast degradation. The injector temperature was set to 250 °C in split mode with a 1:20 ratio. The column temperature program started at an initial temperature of 40 °C followed by a 10 °C·min$^{-1}$ ramp up to a final temperature of 300 °C held for 10 min. The MS settings were identical to the ones described for the EGA experiments and two replicas of each samples were done.

### 2.6. Derivatization-GC–MS

#### 2.6.1. Wet chemistry experiments

In this study, wet chemistry derivatization experiments were performed using N-Methyl-N-(*tert*-butyldimethylsilyl)trifluoroacetamide (MTBSTFA) (98%, Merck) (used on SAM (Mahaffy et al., 2012)) and MOMA (Goesmann et al., 2017)) and *N*,*N*-Dimethylformamide dimethyl acetal (DMF-DMA) (99.0%, Merck) (to be used on MOMA for chiral separation (Goesmann et al., 2017)). 5 mg of the organic/silica mixture were placed in a conic 2 mL glass vial. 35 µL of derivatization reagent were added to the mixture in the vial in order to obtain a supernatant that we could draw from with a syringe for further GC–MS injection. The solution used for DMF-DMA derivatization was heated to 145 °C for 3 min, suitable for *in situ* analysis in space (Freissinet et al., 2010). The MTBSTFA derivatization reagent was mixed with *N*,*N*-Dimethylformamide (DMF) (Merck) in a 4:1 solution (Mahaffy et al., 2012), as employed in the SAM instrumental suite onboard the Curiosity rover. The organic/silica/MTBSTFA/DMF mixture was then heated to 75 °C for 15 min. After heating, the supernatant was collected in an Eppendorf tube, and 1 µL of Naphthalene $d_8$ (99,99% Merck) diluted in DMF (99.0%, Merck) at 5.10$^{-3}$ M was added and used as an internal standard for all the derivatization experiments to compare their respective performances. The solution was centrifuged for 30 s to prevent silica particles from getting stuck in the syringe during the injection. 1 µL of the supernatant was then injected in the instrument. On the SAM and MOMA flight models, the derivatization reagent is contained in dedicated cups or capsules where the sample is dropped. The capsules containing the sample and the reagent are then heated and the volatile products are analyzed through GC–MS (Goesmann et al., 2017; Mahaffy et al., 2012).

#### 2.6.2. Thermochemistry

Thermochemistry experiments were performed using Tetramethylammonium hydroxide (TMAH) diluted at 25% into methanol (Merck) (used on both the SAM and MOMA instruments). 2.5 mg of acid or salts (5.00 mg total) were deposited in the pyrolysis cup. 4 µL of TMAH solution with 1 µL of internal standard (Naphthalene $d_8$) were then added to the solid mixture. The cup containing the sample was introduced in the pyrolysis oven and heated at 600 °C for 30 s under helium flow.

GC–MS analyses for wet chemistry and thermochemolysis experiments were performed under the same conditions as those used for pyrolysis-GC–MS analyses described above.

### 2.7. SAM-flight experiments simulated in the laboratory

Analyses on SAM spare columns were conducted in the laboratory to evaluate the detectability of the products obtained from the pyrolysis

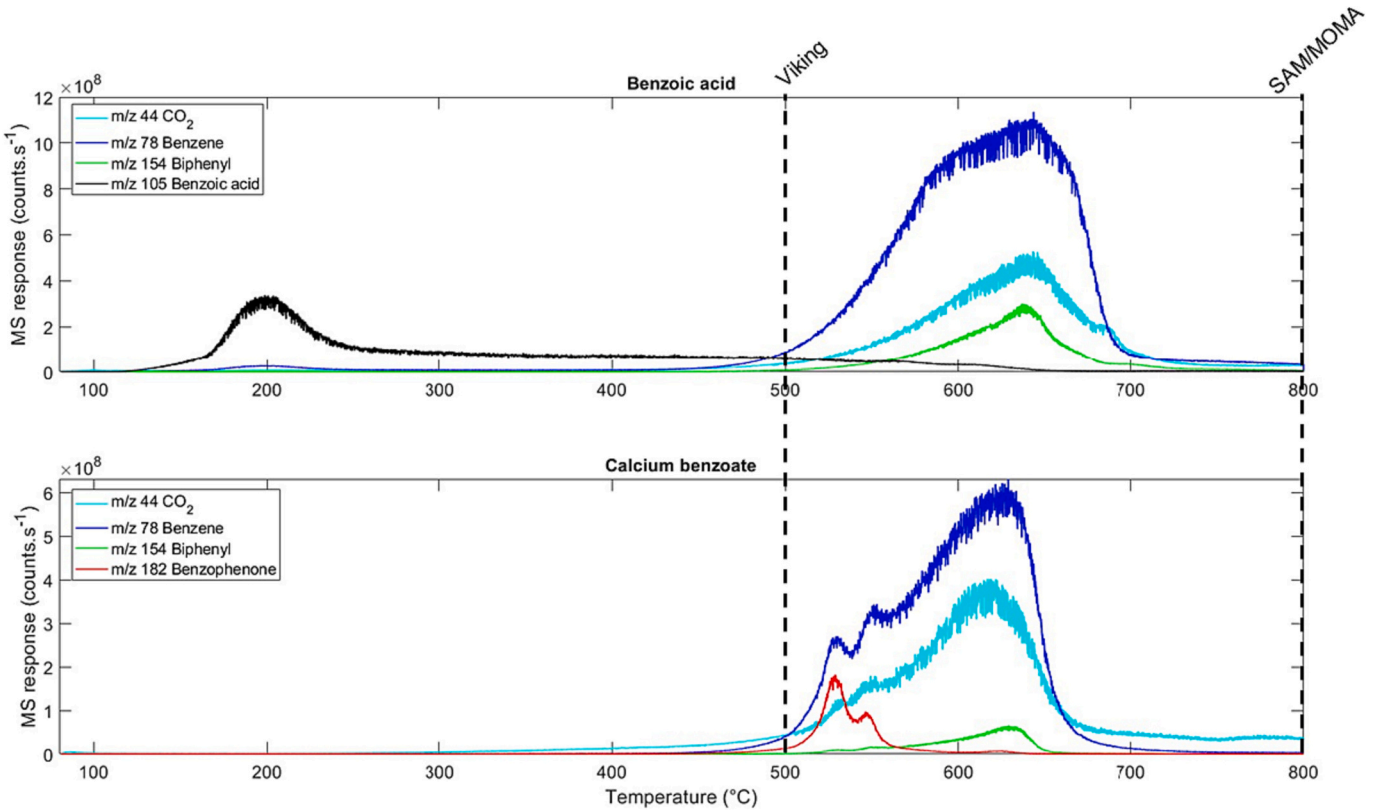


**Fig. 1.** Evolved gas profile of m/z 44 ($CO_2$), m/z 78 (Benzene), m/z 154 (Biphenyl), m/z 105 (Benzoic acid), and m/z 182 (Benzophenone) versus temperature obtained in SAM-like EGA conditions (35 °C·min$^{-1}$ ramp) of a 100:1 fused silica-benzoic acid mixture (top), and a 100:2.3 fused silica-calcium benzoate mixture (bottom). The Viking, SAM and MOMA pyrolysis temperature limits are indicated with dashed lines.

and derivatization experiments of benzoate and phthalate salts if present on the Martian surface. The SAM spare columns kept at the Laboratoire Atmosphères, Observations Spatiales (LATMOS) in France are part of the same set that were integrated into the SAM flight model and allowed to simulate the SAM-like conditions in the laboratory. Among the six columns present on the SAM instrument suite (Mahaffy et al., 2012), two were used in this study: the MXT-5 spare column referred to as GC2 (30 m long; 0.25 mm internal diameter, 0.25 µm stationary phase thickness) (Restek) and the SAM MXT-CLP spare column referred to as GC5 (30 m long; 0.25 mm internal diameter, 0.25 µm stationary phase thickness) (Restek). GC2 was used to reproduce SAM's first *in situ* TMAH thermochemolysis experiment at the Mary Anning (MA) drill site in the Glen Torridon region (Williams et al., 2021). The detection of several compounds of interest in the sample motivated these analyses. GC5 was chosen to evaluate the detectability of the products obtained during the analysis of aromatic carboxylic salts with another SAM spare column. Several *in situ* GC5 analyses have been performed by SAM and performance evaluations of the column in the laboratory showed a good separation efficiency of the tested species regardless of their mass (Millan et al., 2019).

A 60 cm fused silica tubing (0.75 µm/ 190 µm) (SGE) was added to the column end going to the injector. This extension acts as a flow restrictor to allow the regulation of the pressure and mimic the low pressure of the SAM instrument (Millan et al., 2019). A 20 cm silica transfer tube (0.25 mm internal diameter; 0.25 µm stationary phase thickness) was used in the MS transfer line to prevent electrical arcs forming from the presence of a metallic column near the mass spectrometer ion source.

In the flight chromatogram of the Mary Anning (MA) sample obtained with the GC2 column, two species of interest, diphenylmethane and benzoic acid methyl ester, were detected. In order to confirm their identification and assess the possibility to detect other compounds of interest on this column, the temperature parameters as performed *in situ* during the SAM MA experiments were retrieved from the SAM flight data set. Because this flight analysis was performed as a dual column experiment where the samples were analyzed with the SAM MXT-20 column (referred to as GC1) prior to GC2, we took into consideration the opening and closing of the hydrocarbon trap valves that could have allowed chemical species to go through GC2 even before the start of the analysis. Therefore, the GC–MS analyses started with a column temperature of 45 °C for 7 min corresponding to the opening of the hydrocarbon trap valves, followed by a first ramp of 120 °C.min$^{-1}$ to reach 66 °C. Then a second slow rate ramp of 0.3 °C.min$^{-1}$ to 59 °C and finally a third ramp of 10 °C.min$^{-1}$ to reach a final temperature of 232 °C. The analysis was extended at the final temperature for 30 min to ensure the detection of that all the targeted compounds. The pressure was adjusted to match the retention time value of a known molecule, bi-silylated water (BSW), a byproduct of MTBSTFA, identified in the SAM GC2 MA chromatogram.

For GC5, the column temperature program used was identical to the nominal GC5 SAM-flight instrument with an initial temperature of 35 °C for 6.3 min, then 10 °C.min$^{-1}$ rate up to a final temperature of 185 °C. The maximum time of analyses for GC5 is 21 min (Millan et al., 2019) but we extended the run for 40 min at the final temperature to be able to detect all the compounds of interest. The pressure was adjusted on the commercial GC based on the dead time observed on GC5 (Millan et al., 2019).

For all analyses the GC injector was set in a split mode with a 1:20 split ratio. The ion source and transfer line temperatures of the MS were both set at 300 °C, and ions produced by electron impacts (energy of 70 eV) were scanned between masse to charge ratios ($m/z$) of 10 to 585. 1 µL of a solution with the species targeted was then injected in the GC with a syringe.

**Table 1**
Summary of the ranges and maximum temperatures of released benzoic acid (B), calcium benzoate (CaB), phthalic acid (Ph) and calcium phthalate (CaPh) (observed through their main ion) in EGA. N/A: Not Applicable.

| *m/z* | Corresponding molecule | Outagassing temperature range (°C) | | | | Maximum Temperature (°C) | | | |
|---|---|---|---|---|---|---|---|---|---|
| | | B | CaB | Ph | CaPh | B | CaB | Ph | CaPh |
| **44** | **$CO_2$** | 470–800 | 470–800 | 300–800 | 300–800 | 630 | 520 and 680 | 470 | 690 |
| **78** | **Benzene** | 470–800 | 470–800 | N/A | 470–630 | 630 | 630 | N/A | 550 |
| **154** | **Biphenyl** | 500–720 | 500–650 | N/A | N/A | 630 | 630 | N/A | N/A |
| **105** | **Benzoic acid** | 110–620 | N/A | N/A | N/A | 200 | N/A | N/A | N/A |
| **148** | **Phthalic acid** | N/A | N/A | 180–280 | N/A | N/A | N/A | 230 | N/A |
| **182** | **Benzophenone** | N/A | 470–590 | N/A | 470–600 | N/A | 530 and 550 | N/A | 560 |

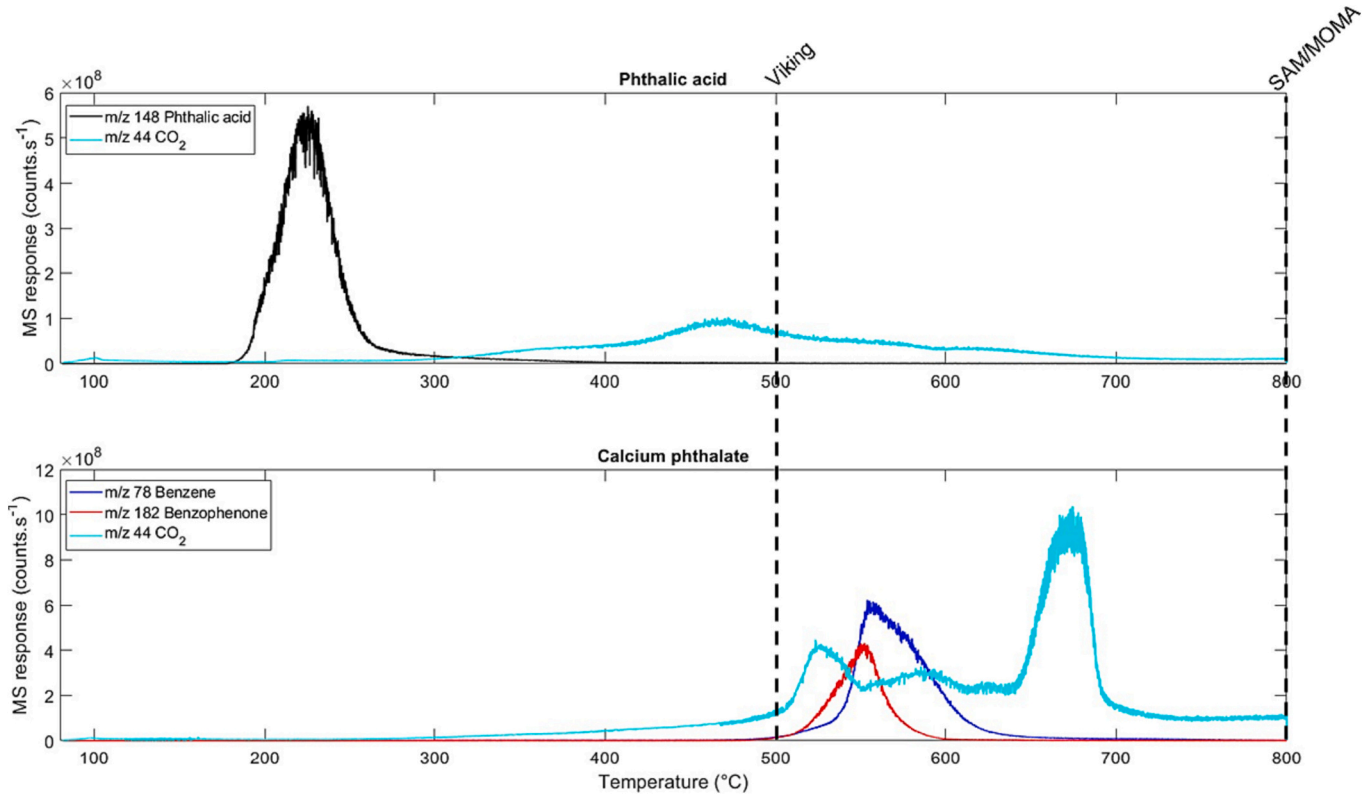


**Fig. 2.** Evolved gas profile for *m/z* 44 ($CO_2$), m/z 78 (Benzene), m/z 148 (Phthalic acid), and m/z 182 (Benzophenone) *versus* temperature obtained in SAM-like EGA conditions (35 °C.min$^{-1}$ ramp) of a 100:1 fused silica-phthalic acid mixture (top), and a 100:1.2 fused silica-calcium phthalate mixture (bottom). The Viking, SAM and MOMA pyrolysis temperature limits are indicated with dashed lines.

## 3. Results

### 3.1. EGA

#### 3.1.1. Thermal behavior of benzoic acid compared to calcium benzoate

Fig. 1 represents the evolution of the main ions detected during the EGA of benzoic acid and its associated salt, calcium benzoate. We observed that benzoic acid released gases within two distinct temperature ranges: the first release occurred around 110 °C and reaches a maximum around 200 °C with a tail reaching up to 620 °C. The corresponding organic compound is benzoic acid itself identified from its mass spectrum and characterized by its parent molecular ion (*m/z* 105). The second gas release starts at higher temperatures and ranges from 470 °C to 800 °C, with a maximum at ~630 °C. The signal is more intense than the first peak, indicating that only a small amount of benzoic acid was released at lower temperatures. Three main ions contribute to the second release: *m/z* 44, *m/z* 78 and *m/z* 154 corresponding to $CO_2$, benzene and biphenyl, respectively, which were identified *via* their mass spectra. $CO_2$ and benzene are products of the decarboxylation of benzoic acid, and biphenyl results from the interaction of benzene rings. The temperature ranges at which each compound evolve can be found in Table 1.

For calcium benzoate, no low-temperature benzoic acid release was observed, indicating that no hydrogenation of the benzoate anion occurred during the heating of the sample. However, as for benzoic acid, we observe that gases are released from the sample mainly within the temperature range 470 °C to 800 °C. Most of the chemical species contributing to this signal are the same as those identified for benzoic acid, *i.e.* $CO_2$, benzene and biphenyl. However, the EGA of calcium benzoate reveals the presence of an additional species detected in the range 470 °C and 590 °C, with a characteristic ion *m/z* 182 corresponding to benzophenone. This result is in agreement with a study published by Dabestani et al. (2005). The presence of two maxima in the corresponding peak can be explained by the presence of two benzoic acid molecules complexed with $Ca^{2+}$ which ensures electronegativity. The first molecule is transformed into benzophenone followed by the second molecule at slightly higher temperature.

#### 3.1.2. Thermal behavior of phthalic acid compared to calcium phthalate

Fig. 2 represents the evolution of the main ions of phthalic acid and

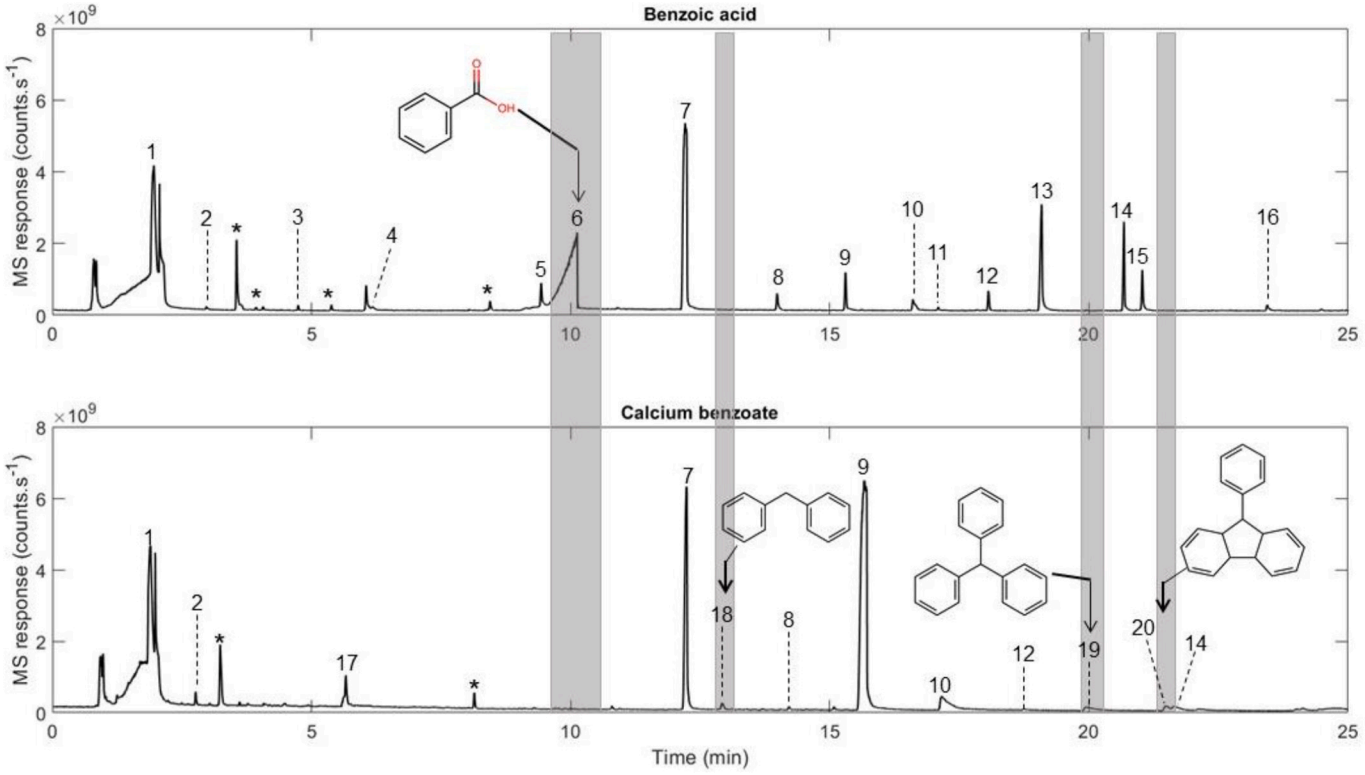


**Fig. 3.** Chromatograms obtained from the pyrolysis (35 °C·min$^{-1}$ ramp, up to 800 °C) of benzoic acid (top) and calcium benzoate (bottom) at 1 wt% in fused silica, in SAM-like pyrolytic conditions (35 °C·min$^{-1}$). The grey shading corresponds to molecules unique to the pyrolysis of the acid or unique to that of the salt. (*)artifact of the column (stationary phase bleeding), (1) benzene, (2) toluene, (3) styrene, (4) phenol, (5) naphthalene, (6) benzoic acid, (7) biphenyl, (8) dibenzofuran, (9) benzophenone, (10) fluorenone, (11) Fluorene, methylene-, (12), (14), and (15) terphenyl isomers, (13) anthracenedione, (16) benzanthracene, (17) trimethylbenzene, (18) diphenylmethane, (19) triphenylmethane, (20) 9H-Fluorene, phenyl-.

its corresponding salt, calcium phthalate in EGA. We observed that phthalic acid produced a single major peak corresponding to the molecular ion at *m/z* 148 in the relatively low temperature range 180 °C to 280 °C, with a maximum around 230 °C (Table 1). No other major species were detected. Release of $CO_2$ (*m/z* 44) from 300 to 800 °C with a maximum around 470 °C was also observed with a lower intensity (~6 times lower than the phthalic acid peak's maxima). This $CO_2$ release could come from the decarboxylation of the acid leading to the formation of species such as benzoic acid or benzene. The masses of these two molecules were found in the EGA of phthalic acid, but at level of abundance close to the limit of detection ($10^6$).

The calcium phthalate did not produce phthalic acid. However, we observed species evolving at high temperatures. Three main ion contributors were identified. As observed in the EGA of calcium benzoate, we identified a peak evolving from 470 °C to 600 °C with a maximum at 560 °C corresponding to benzophenone (*m/z* 182). Benzophenone co-evolved with the release of benzene (m/z 78) between 470 °C to 630 °C with a maximum at 560 °C. A major $CO_2$ release is observed between 300 °C and 800 °C with two maxima: the first peak around 520 °C and a higher intensity peak around 680 °C. The release of benzene and $CO_2$ are related to the decarboxylation of the salt.

The evolution of $CO_2$ (m/z 44) is different for the phthalic acid and calcium phthalate. In the EGA of phthalic acid, the $CO_2$ peak is widely spread throughout the thermal range at low intensities, whereas, for calcium phthalate, $CO_2$ has a higher degassing intensity and higher temperatures. The absence of organic compounds during the $CO_2$ evolution in the EGA of phthalic acid and around 670 °C for calcium phthalate could either mean that the organic molecules formed are below the detection level of our instruments or that there is a complete degradation of the compound resulting only in carbon dioxide in that temperature range.

### 3.2. Pyrolysis GC–MS

#### 3.2.1. Pyrolysis in slow heating mode (35 °C.Min$^{-1}$) (SAM-like)

*3.2.1.1. Benzoic acid versus calcium benzoate.* Fig. 3 shows that pyrolysis of benzoic acid under SAM-like conditions produced a variety of aromatic compounds. The major organic molecules observed in EGA, *i.e.* benzene, benzoic acid and biphenyl, are also detected in GC–MS as the most abundant compounds. The peak shape for the benzoic acid (Fig. 3, top chromatogram, peak 6) is typical of column overloading resulting from a poor solubility of the molecule in the stationary phase and/or a quantitative saturation.

Fewer compounds were produced from the pyrolysis of calcium benzoate compared to benzoic acid. This is likely an indication of a higher thermal stability of the salt compared to benzoic acid (from the EGA data). We retrieved the major species detected in EGA, *i.e.* benzene, biphenyl and benzophenone. As expected, the parent molecule, benzoic acid, identified among the most abundant compounds in the chromatogram of the acid, was not detected in the pyrolysis of calcium benzoate. Instead, calcium benzoate evolved another major compound, benzophenone (Fig. 3, peak 7), as predicted by the EGA results, which was found in much lower concentration in the chromatogram of the acid (area of the benzophenone peak/area of the biphenyl peak = 2.1 for the salt compared to 0.8 for the acid). The salt also produced additional molecules that were not detected in the chromatogram of benzoic acid such as diphenylmethane, triphenylmethane and phenyl fluorene (Fig. 3, bottom chromatogram, peak 18, 19 and 20, respectively).

*3.2.1.2. Phthalic acid versus calcium phthalate.* Fig. 4 showed that phthalic acid did not evolve many byproducts in ramp pyrolysis conditions and the major product detected was phthalic acid itself (Fig. 4, top

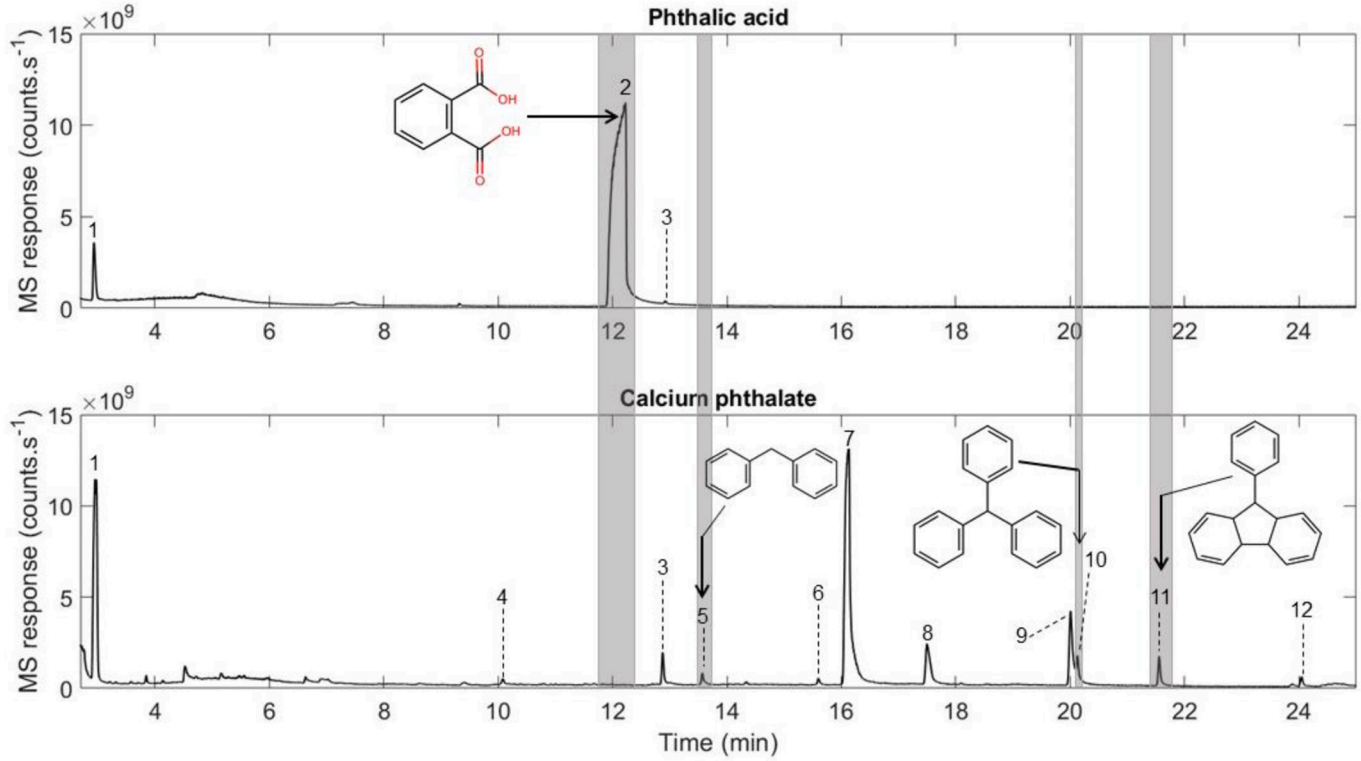


**Fig. 4.** Chromatograms obtained from the pyrolysis (35 °C·min$^{-1}$ ramp, up to 800 °C) of phthalic acid (top) and calcium phthalate (bottom) at 1 wt% in fused silica in SAM-like pyrolytic conditions. The grey shading corresponds to molecules unique to the pyrolysis of the acid or unique to that of the salt. (1) benzene, (2) phthalic acid, (3) biphenyl, (4) naphthalene, (5) diphenylmethane, (6) fluorene, (7) benzophenone, (8) fluorenone, (9) anthracenedione, (10) triphenylmethane, (11) fluorene, phenyl-, (12) anthracene, phenyl-.

chromatogram, peak 2). This is consistent with the EGA results (Fig. 2). On the other hand, phthalic acid was not detected when calcium phthalate was pyrolyzed in SAM-like heating conditions, as expected from the EGA results. However, several byproducts were generated during the ramp pyrolysis of calcium phthalate with benzene and benzophenone as the two major products (Fig. 4, bottom chromatogram, peak 1 and 7, respectively) as well as other compounds such as fluorenone or anthracenedione (Fig. 4, bottom chromatogram, peak 8 and 9, respectively). The EGA results suggest that calcium phthalate is stable under low temperature conditions, and that the byproducts detected in GC–MS were formed through cleavage when high temperature (> 500 °C) was reached. As in the pyrolysis of calcium benzoate, diphenylmethane, triphenylmethane and phenyl fluorene were identified as characteristic products of the degradation of calcium phthalate (Fig. 4, bottom chromatogram, peak 5, 10 and 11, respectively).

### 3.2.2. *Pyrolysis in flash 500 °C heating mode (Viking-like)*

*3.2.2.1. Benzoic acid versus calcium benzoate.* Fig. 5 shows the stark difference between the compounds detected with benzoic acid and calcium benzoate during flash pyrolysis at 500 °C. In the chromatogram of the acid, the parent molecule, benzoic acid (Fig. 5, top chromatogram, peak 3), is detected as a major compound as predicted by the EGA results (Fig. 1). Other molecules were detected in high abundance such as benzene, phenol, and biphenyl (Fig. 5, top chromatogram, peak 1, 2 and 4, respectively).

Benzoic acid was not detected when calcium benzoate was flash pyrolyzed to 500 °C. Overall, calcium benzoate did not evolve many gaseous products in flash 500 °C conditions. The major compound observed is benzene (Fig. 5, top chromatogram, peak 1), in agreement with EGA, showing that this is the major compound among those observed to be released above 470 °C. The absence of byproducts is related to the evolution temperature of calcium benzoate species, which as shown by the EGA, evolved at temperatures above 500 °C.

*3.2.2.2. Phthalic acid versus calcium phthalate.* Phthalic acid was not detected when calcium phthalate was pyrolyzed in fast heating mode to 500 °C whereas it was the major compound observed during the pyrolysis of the acid (Fig. 6, top chromatogram, peak 4), as expected from EGA results. The flash pyrolysis of calcium phthalate to 500 °C generated benzophenone as the major product, followed by fluorenone and anthracenedione (Fig. 6, bottom chromatogram, peak 5, 6 and 7, respectively). The Total Ion Current (TIC) chromatogram of calcium phthalate represented in Fig. 6 did not allow the detection of benzene. However, its presence was confirmed through selected-ion monitoring (SIM) mode by selecting the base peak (*m/z* 78). Moreover, diphenylmethane and triphenylmethane were not observed in the chromatogram of the salt, though we detected phenyl fluorene as a pyrolysis byproduct of aromatic carboxylic salts pyrolysis as mentioned above (Fig. 6, bottom chromatogram, peak 8).

### 3.2.3. *Pyrolysis in flash 800 °C heating mode (MOMA-like)*

*3.2.3.1. Benzoic acid versus calcium benzoate.* Fig. 7 shows that benzoic acid was more degraded at high flash pyrolysis temperature (800 °C), and therefore was not the major compound detected contrary to what was observed in the two previous pyrolysis conditions for the acid (Fig. 7, top chromatogram, peak 3). Moreover, the major compounds in the chromatograms of benzoic acid flash-pyrolyzed to 800 °C were benzene and biphenyl (Fig. 7, top chromatogram, peak 1 and 5, respectively) as seen in EGA. For calcium benzoate the parent molecule was not detected in the chromatogram of calcium benzoate but produced benzene and biphenyl as major compounds (Fig. 7, bottom chromatogram, peak 1 and 5, respectively) as described in the EGA

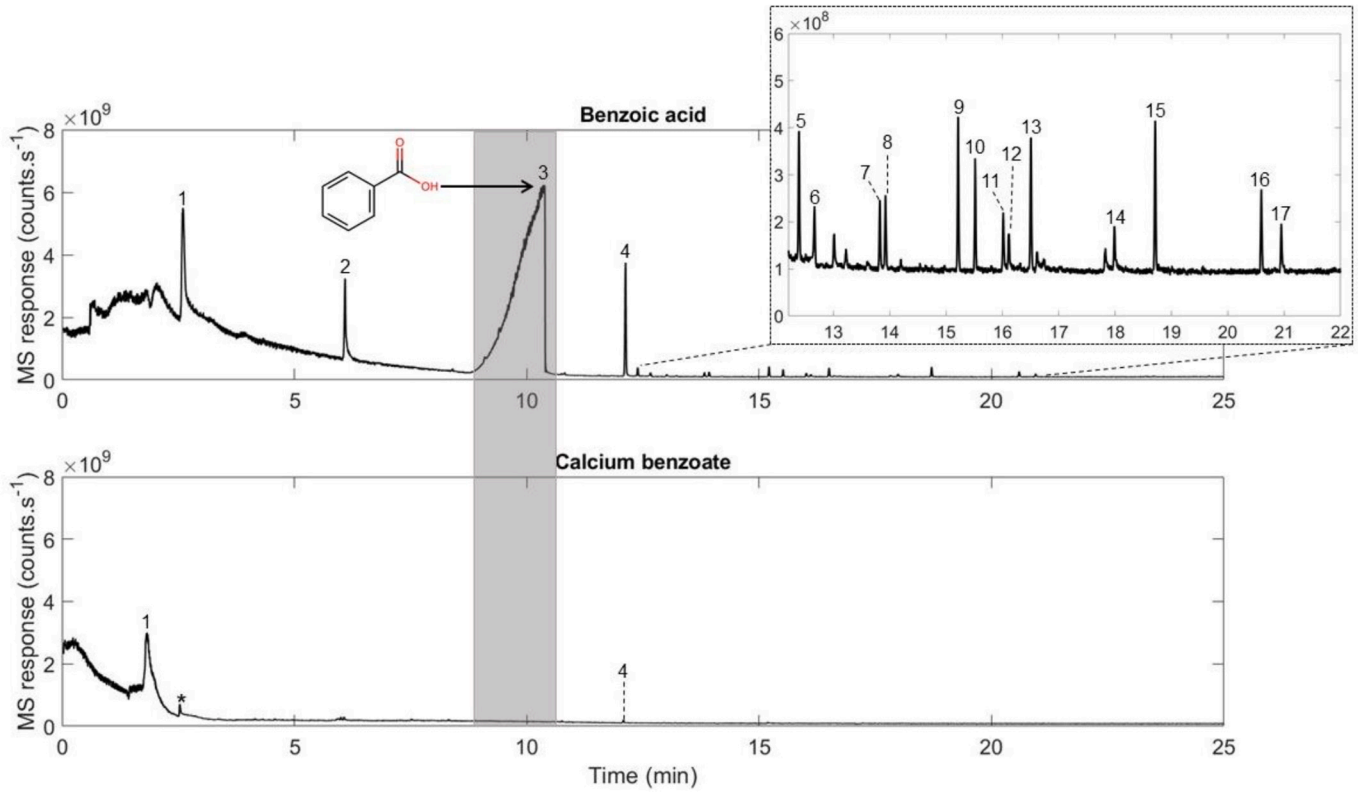


**Fig. 5.** Chromatograms obtained from the flash pyrolysis (500 °C) of benzoic acid (top) and calcium benzoate (bottom) at 1 wt% in fused silica. The grey shading corresponds to molecules unique to the pyrolysis of the acid or unique to that of the salt. (*) artifact of the column (stationary phase bleeding), (1) benzene, (2) phenol, (3) benzoic acid, (4), biphenyl, (5) diphenyl ether, (6) phenylpropenal, (7), (11), and (12) hydroxybiphenyl (isomers), (8) dibenzofuran, (9) benzophenone, (10) benzoic acid, phenyl ester, (13) 9H-Fluoren-9-one, (14), (16), and (17) terphenyl (isomers), (15) 4-Hydroxy-9-fluoreneone.

experiments. The low intensity of the benzophenone peak (Fig. 7, bottom chromatogram, peak 8) in the chromatogram can be explained by side-reactions happening at high temperature during flash pyrolysis. Moreover, similar byproducts are formed between the acid and the salts but with intensity differences. Benzoic acid produced a much higher yield of terphenyl isomers (Fig. 7, top chromatogram, peak 17 marked with black diamonds), as well as more intense peaks of naphthalene, dibenzofuran, fluorenone, anthracene or Benzanthracene. Moreover, we identified the formation of several quaterphenyl isomers (Fig. 7, top chromatogram, peaks 12, 14 and 15) during the pyrolysis of the benzoic acid which were absent with the calcium benzoate. Calcium benzoate did not produce the characteristic byproducts diphenylmethane, triphenylmethane and phenyl fluorene at flash 800 °C.

*3.2.3.2. Phthalic acid versus calcium phthalate.* As previously shown with the benzoate couple, the parent molecule in the phthalic acid chromatogram is present (Fig. 8, top chromatogram, peak 11) but at much lower intensity compared to the previous conditions used which is likely due to the velocity (flash) and the high temperature of pyrolysis applied here. A high number of molecules were detected including benzene and biphenyl resulting from the decarboxylation of benzoic acid and the recombination of benzene rings (Fig. 8, top chromatogram, peak 1 and 13, respectively). Phenol was also detected in both chromatograms of phthalic acid obtained after flash pyrolysis at 500 °C and 800 °C, but it was not detected in ramp pyrolysis. This further confirms that the type of pyrolysis (flash or ramp) applied can contribute to different reactional pathways of the molecules.

After the flash pyrolysis (800 °C) of calcium phthalate, phthalic acid was not detected but numerous byproducts were produced. Among them, benzene, biphenyl, and benzophenone were detected (Fig. 8, bottom chromatogram, peak 1, 13 and 19, respectively). Finally, as observed in the chromatogram of both aromatic calcium salts in SAM-like conditions (35 °C.min$^{-1}$), diphenylmethane, triphenylmethane and phenyl fluorene were detected as characteristic products of pyrolysis of the salt as they were not present in the chromatogram of phthalic acid (Fig. 8, bottom chromatogram, peak 40, 42 and 43, respectively).

### 3.3. Wet chemistry derivatizations

A comparison of the derivatized species and their yield for all three derivatization reagents was performed to assess the behavior of calcium salts *versus* carboxylic acids in wet chemistry experiments (Fig. 9). We observed that both the acid and the salt can be derivatized with MTBSTFA, DMF-DMA and TMAH and that they both generated the same derivatized molecules under a given derivatization reagent. The derivatization with DMF-DMA and TMAH formed benzoic acid methyl ester with the benzoic acid and calcium benzoate, and dimethyl phthalate with phthalic acid and calcium phthalate. With MTBSTFA, benzoic acid and calcium benzoate both derived benzoic acid *tert*-butyldimethylsilyl ester, and phthalic acid and calcium phthalate both derived phthalic acid, bis tert-butyldim ethylsilyl ester. We did not detect other derivatized molecules than the one mentioned, and the usual byproducts of the derivatization reagents.

The derivatization products of the aromatic carboxylic salts were detected with the three derivatization reagents. With MTBSTFA, both calcium benzoate and calcium phthalate produced a higher abundance (~ + 42% and + 24%, respectively) of derivatized byproducts than their acid counterpart. With DMF-DMA, the derivatization products of the calcium salts were detected with both derivatization reagents but in significantly lower abundance than that of the acids, (~ 84% and - 99%, respectively). Finally, with TMAH, benzoic acid and calcium phthalate had the same derivatization yield, whereas phthalic acid derivatized better (~+ 30%) than calcium phthalate.

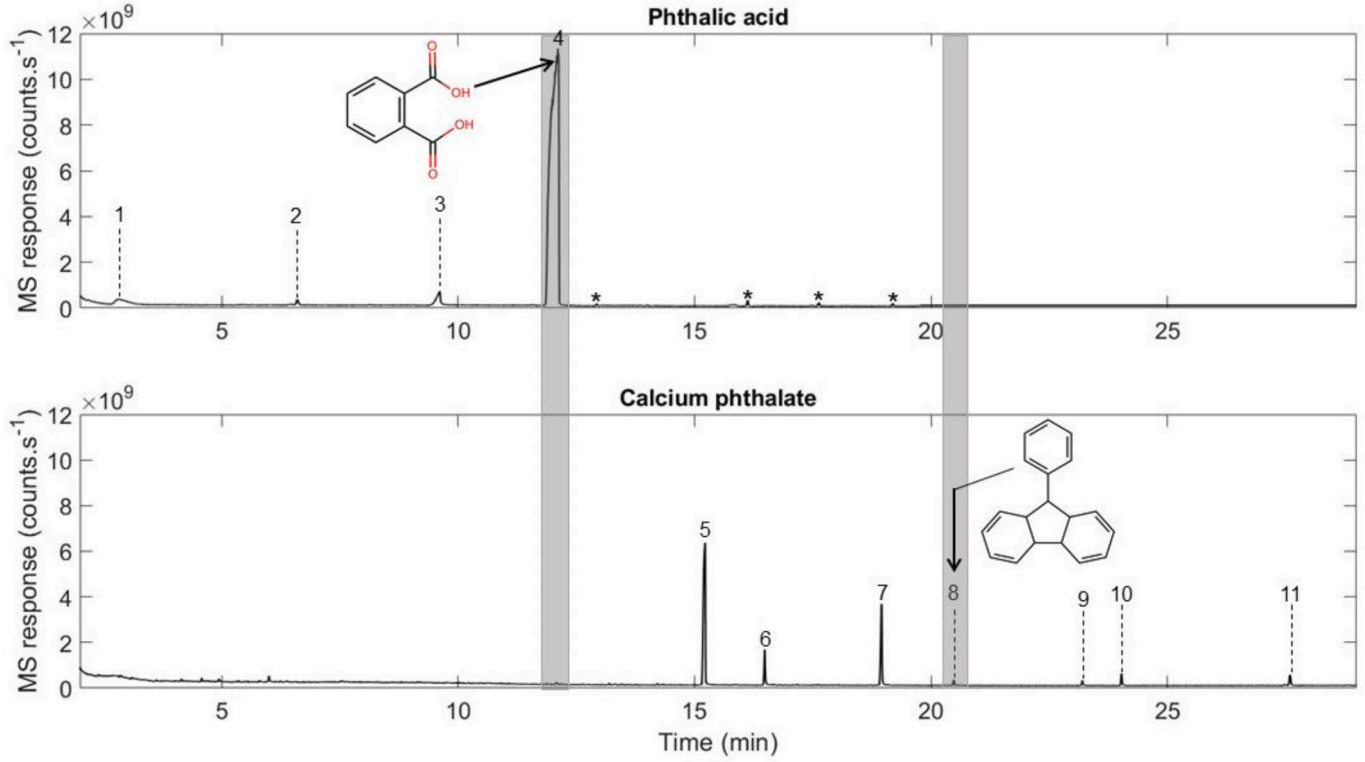


**Fig. 6.** Chromatograms obtained from the flash pyrolysis (500 °C) of phthalic acid (top) and calcium phthalate (bottom) at 1 wt% in fused silica. The grey shading corresponds to molecules unique to the pyrolysis of the acid or unique to that of the salt. (*) artifact of the column (stationary phase bleeding), (1) benzene, (2) phenol, (3) benzoic acid, (4) phthalic acid, (5) benzophenone, (6) fluorenone, (7) anthracenedione, (8) fluorene, phenyl, (9) and (10) unidentified compound, (11) anthracene, diphenyl-.

The abundance of the derivatized molecules is substantially higher for both the acid and the salt with MTBSTFA compared to DMF-DMA. However, we were not able to compare the derivatization efficiency of TMAH with MTBSTFA and DMF-DMA as the protocols used for thermochemistry and wet chemistry were different.

### 3.4. SAM versus laboratory experiments

Previous analyses conducted on the SAM instrument were reviewed to see if some of the species relevant to the identification of aromatic salts, as mentioned in this study, had been detected. Two species relevant to this study were identified in the Mary Anning (MA) sample by SAM: benzoic acid methyl ester, a possible thermochemolysis product of benzoate salts with TMAH and diphenylmethane, one of the characteristic product of pyrolysis of benzoates and phthalates as observed in this study. The mass to charge ratio ($m/z$) of benzoic acid methyl ester and diphenylmethane, $m/z$ 105 and $m/z$ 167, respectively were retrieved from the SAM chromatogram (Fig. 10, top red chromatogram). The laboratory chromatogram (Fig. 10, bottom black chromatogram) shows that both species are within the same retention time range as in the SAM chromatogram, providing a robust identification. However, benzophenone and triphenylmethane were not identified in the Mary Anning sample but could be detected with GC2 if they were present above their limit of detection. Finally, phenyl fluorene would elute beyond the end of the SAM run and would not have been detectable in Mary Anning, even if present.

However, it is important to note that while the temperature programs and pressure of the SAM GC2 column were simulated in the laboratory, slight differences remain as the flight and laboratory setups are not strictly identical. The shifts observed between the peaks of the molecule in the SAM and laboratory analyses could be explained by several factors: (1) the temperature profile variations in the flight model is that the columns' temperature control is less precise due to the heating technique employed (Millan et al., 2019; Millan et al., 2016). (2) The lack of adsorption injection trap (IT) prior to the GC2 column on the SAM instrument. However, its absence upstream the GC2 column indicates that all the compounds released during pyrolysis have different retention times, thus making it difficult to match with laboratory measurements despite pressure calibration. (3) Finally, the SAM flight and spare column might have aged differently which could also play a role in the release of organic molecules.

To test the capability of another SAM column to detect species of interest for the identification of aromatic calcium salts, the SAM GC5 spare column was used. In Fig. 11, the retention times of products of interests from the thermal degradation and derivatization of organic calcium salts are shown, within the conditions of a typical GC5 analysis. The maximum duration of a typical SAM GC5 *in situ* analysis is of 21 min. In this chromatogram, only benzoic acid methyl ester elutes within 21 min. The other species analyzed (diphenylmethane, benzophenone, triphenylmethane and phenyl fluorene), would elute after the end of the SAM GC–MS analysis, and thus would not be detected even if present in a Martian sample.

## 4. Discussion

Our laboratory investigations have demonstrated the utility of combining EGA and GC–MS analyses, as well as thermal extraction (pyrolysis) and wet chemistry (derivatization) techniques for the identification of aromatic organic salts linked to calcium on Mars. The results suggest that benzoic acid and phthalic acid, if present in the soil of Mars, could be readily identified through the detection of the acid itself, with EGA and pyrolysis-GC–MS techniques. However, their salt counterpart, calcium benzoate and calcium phthalate, cannot be detected because of their refractory nature. Indeed, calcium benzoate and calcium phthalate

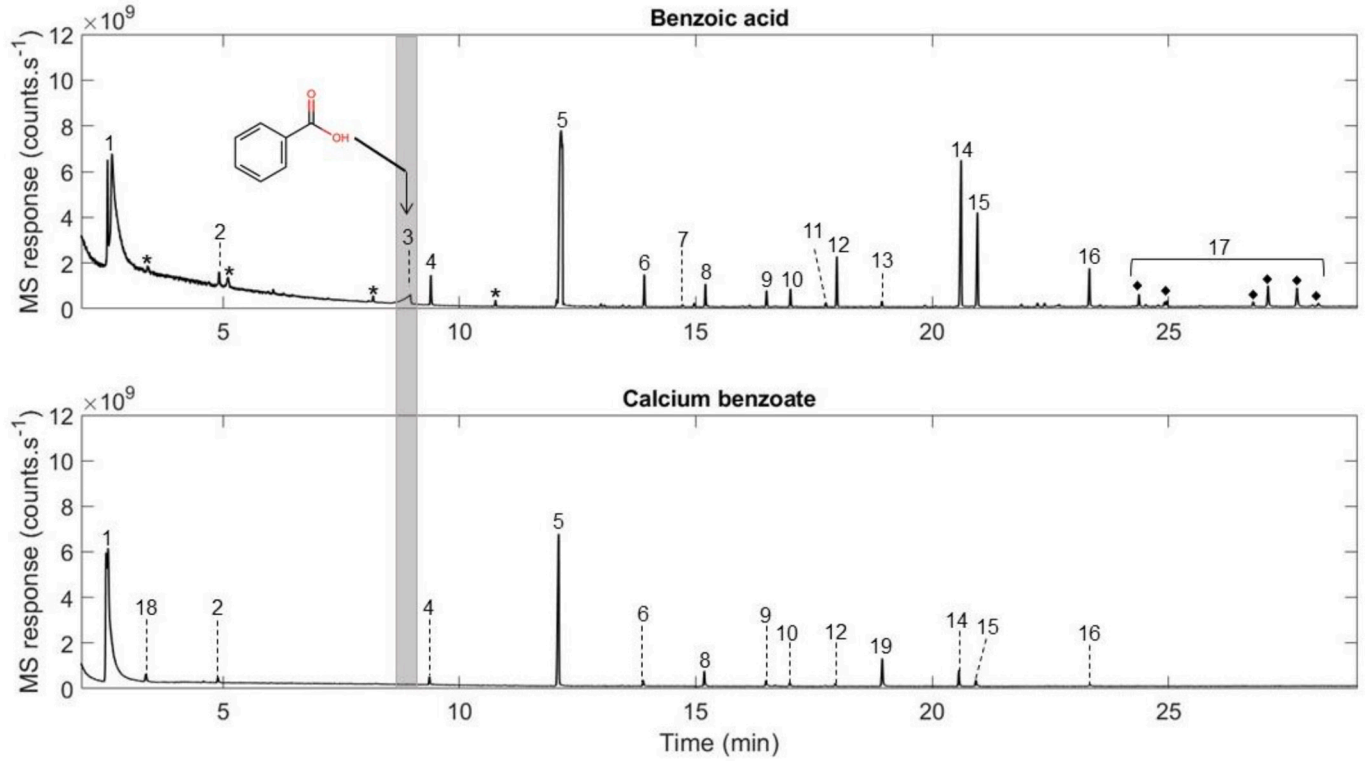


**Fig. 7.** Chromatograms obtained from the flash pyrolysis (at 800 °C) of benzoic acid and calcium benzoate diluted at 1 wt% in fused silica. The grey shading corresponds to molecules unique to the pyrolysis of the acid or unique to that of the salt. (*) artifact of the column (stationary phase bleeding), (1) benzene, (2) styrene, (3) benzoic acid, (4) naphthalene, (5) biphenyl, (6) dibenzofuran, (7) fluorene, (8) benzophenone, (9) fluorenone, (10) anthracene, (11) 1H-Indene, 1-(phenylmethylene)-, (12), (14), and (15) terphenyl isomers, (13) phenylnaphthalene, (16) benzanthracene, (17) quaterphenyl isomers (peaks indicated by the black diamonds), (18) toluene, (19) anthracenedione.

possess strong ion-dipole intermolecular forces as well as higher molecular weight of the salt (benzoic acid MW = 122 g·mol$^{-1}$/Calcium benzoate MW = 282 g·mol$^{-1}$ and phthalic acid MW = 166 g·mol$^{-1}$/ calcium phthalate MW = 204 g·mol$^{-1}$), both contributing factors for the decreased volatility of the organic salt.

### 4.1. EGA

The outgassing of the thermal decomposition products of the calcium salts only occurred at temperatures higher than 470 °C. Thus, only instruments with a sufficient heating capability (> 500 °C) would be able to detect the degradation products of the salts if present in a sample. Therefore, the Viking pyrolysis system would be insufficient and could explains the lack of detection of such organic compounds as discussed by Benner et al. (2000). At high temperature both organic calcium salts released benzophenone in high abundance with both EGA and GCMS modes. Benzophenone could be used as a qualitative clue to the presence of aromatic carboxylic salts. However, the gases produced by the thermal decomposition of calcium phthalate were similar to those produced from calcium benzoate. Thus, identifying the specific parent salt in a sample could be difficult except that calcium benzoate also produced biphenyl which is not observed with calcium phthalate. The presence of biphenyl combined to benzophenone in EGA could thus be a qualitative way to discriminate between these two aromatic organic salts.

### 4.2. Pyrolysis-GC–MS

In GC–MS, the presence of calcium benzoate and calcium phthalate could only be inferred through the identification of several byproduct characteristic of the degradation of the salts during pyrolysis. For both carboxylic acid couples studied, the acid and the salt did not follow the same degradation pathway resulting in differences in the species detected. Several byproducts characteristic of the thermal degradation of both aromatic calcium salts have been identified in GC–MS: benzophenone, diphenylmethane, triphenylmethane, and phenyl fluorene. Except for benzophenone, which was also identified in EGA, the other compounds are seen in GC–MS only, due to the separation power of the GC and a better limit of detection, which allows a better identification of the compounds. This confirms the complementary nature of the EGA and GC–MS techniques, the former giving precious information on the decomposition temperatures and pathways of the original compounds, and the latter to strictly identify compounds with a higher sensitivity. Dabestani et al. (2005) described the reaction pathway of calcium benzoate and suggested that the initial decarboxylation of the benzoate salt leads to the formation of phenyl anion as the key intermediate. The reaction of the phenyl anion with alkali benzoate generates benzophenone as a major product which further reacts to form other compounds such as diphenylmethane, triphenylmethane or phenyl fluorene. A similar behavior between calcium phthalate and benzoate suggests that the pyrolysis of both salts proceeded *via* a similar anionic reaction pathway. Thus, if the parent organic ion of calcium phthalate is not detected, characteristic products of thermal evolution are clearly identified and they could be used as tracers of calcium benzoate and calcium phthalate on Mars despite not being able to discriminate between the mono- and di-acid, with pyrolysis-GC–MS alone.

Diphenylmethane was detected as a Tenax byproduct with and without perchlorate in a study by Buch et al., (2019). This same study showed that benzophenone was also formed as a Tenax byproduct in the presence of perchlorate. Because the degassing temperature of both calcium salts is consistent with the degassing temperature of calcium perchlorate (Millan et al., 2020) and magnesium perchlorate (Clark et al., 2020) into HCl, $O_2$ and $Cl_2$, oxychlorine reacting with Tenax could

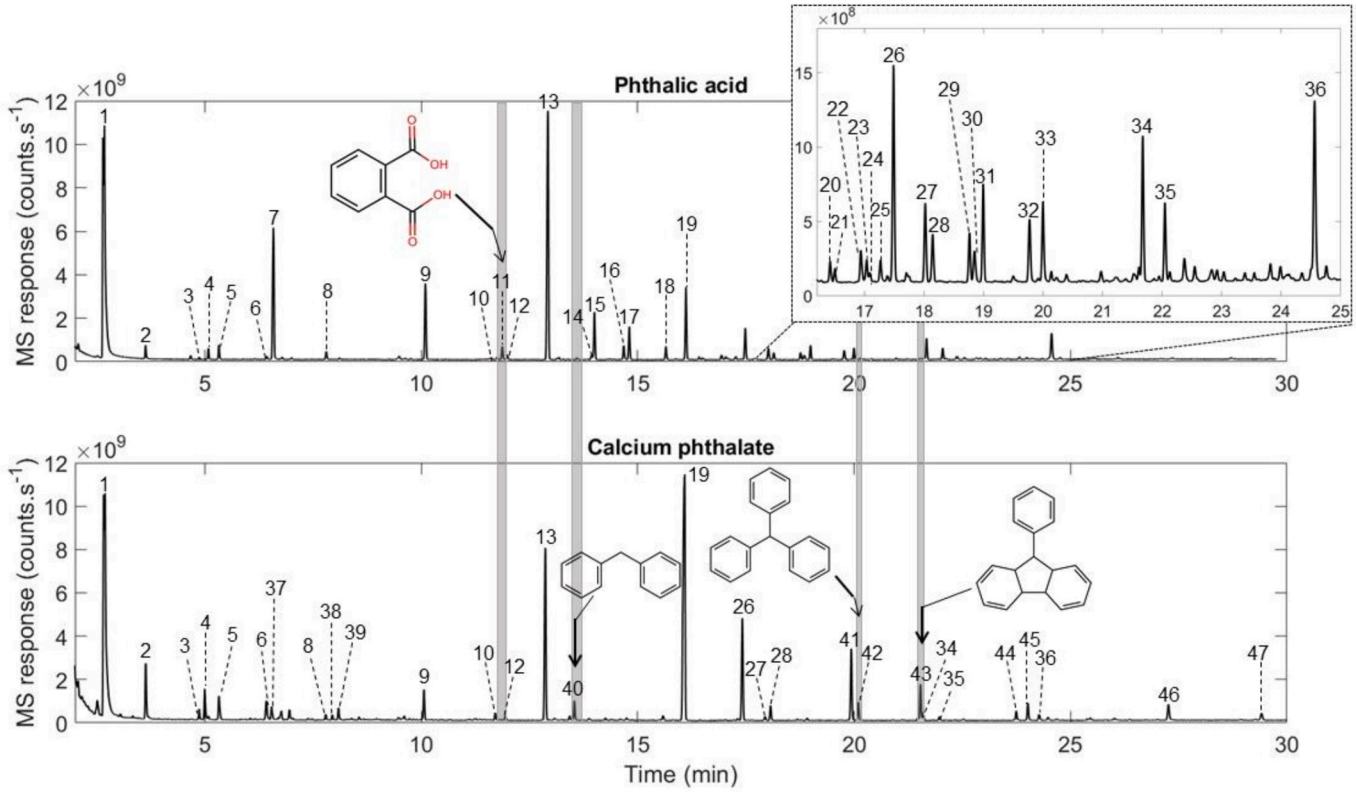


**Fig. 8.** Chromatograms obtained from the flash pyrolysis (at 800 °C) of phthalic acid (top) and calcium phthalate (bottom) diluted at 1 wt% in fused silica The grey shading corresponds to molecules unique to the pyrolysis of the acid or unique to that of the salt. (*) artifact of the column (stationary phase bleeding), (1) benzene, (2) toluene, (3) ethylbenzene, (4) phenylethyne, (5), styrene, (6) benzaldehyde, (7) phenol, (8) benzene, propynyl, (9) naphthalene, (10) and (12) methylnaphthalene (isomers), (11) phthalic acid, (13) biphenyl, (14) acenaphthylene, (15) biphenylene, (16), (22), and (23) hydroxybiphenyl (isomers), (17) dibenzofuran, (18) fluorene, (19) benzophenone, (20) benzoic acid, phenyl ester, (21) diphenylacetylene, (24) stilbene, (25) Methanone, (2-hydroxyphenyl)phenyl-, (26) fluorenone, (27) anthracene, (28) phenanthrene, (29) anthracene, ethynyl-, (30) xanthone, (31), (34), and (35) terphenyl (isomers), (32) 4-hydroxy-9-fluorenone, (33) phenylnaphthalene, (36) benzanthracene, (37) xylene, (38) trimethylbenzene, (39) Benzene, ethyl-dimethyl-, (40) diphenylmethane, (41) anthracenedione, (42) triphenylmethane, (43) fluorene, phenyl-, (44) phenylanthracene, (45) Methanone, [1,1′-biphenyl]-4-ylphenyl-, (46) benzo fluoranthene, (47) anthracene, diphenyl-.

be the source of diphenylmethane or benzophenone if detected *in situ* with SAM. So far, none of these molecules have been detected in the samples analyzed by SAM except for diphenylmethane which was identified at the Mary Anning drill site in the Glen Torridon region (Williams et al., 2021). However, we have demonstrated that all these molecules could have been detected if they were present in the Martian soil with the GC2 SAM column, except phenyl fluorene which would elute after the end of the SAM analysis time (Fig. 10). The absence of benzophenone in the Mary Anning chromatogram is a definitive clue that aromatic calcium salts are not present in the MA sample. To detect phenyl fluorene, the temperature ramp could be increased, which would shorten the elution time of the compounds making the detection of phenyl fluorene more likely in future runs where the presence of aromatic organic salts was to be suspected. With the SAM GC5 column, however, the detection of aromatic salt byproducts is unlikely as they should all elute after the maximum time of analysis for this column in SAM temperatures conditions (21 min). A longer analysis would be required in order to identify some of the species in case a clue of the presence of aromatic carboxylic salts was detected with EGA and/or derivatization. This shows the importance to have multiple columns on flight instruments and the predictive results such as EGA, which can help predict the detection of refractory compounds. This work should be applied to MOMA columns as well.

The slow pyrolysis ramp (35 °C·min$^{-1}$) used on the SAM instrument seems to be more appropriate to detect the indirect clues of the presence of aromatic calcium salts through characteristic compounds, compared to the flash pyrolysis used on the MOMA instrumental set-up. Indeed, the results showed that in SAM-like pyrolysis conditions with a slow rate ramp of 35 °C·min$^{-1}$, diphenylmethane, triphenylmethane and phenyl fluorene were released. Results gathered from the flash 800 °C pyrolysis experiments showed that both carboxylic acids and their salt counterpart produced similar byproducts which can render their discrimination difficult especially due to the low intensity of the parent molecule in the chromatograms of the acids. Calcium phthalate produced the three characteristic byproducts diphenylmethane, triphenylmethane and phenyl fluorene that, could serve as indirect clue for the identification of phthalate if present above the detection limit of the flight instruments. However, these compounds were not observed in the chromatogram of calcium benzoate making its identification difficult. The kinetic of formation of benzoate products might be slower than for phthalates, which could explain the lack of detection of the characteristic products of calcium benzoate at flash 800 °C. Therefore, MOMA pyrolysis experiments would benefit from step pyrolysis temperatures instead of a direct flash 800 °C pyrolysis to help distinguish features specific to the degradation of both the salts and their acid form. Moreover, if the presence of aromatic carboxylic salts was suspected in a Martian sample, a slower temperature ramp (< 200 °C.min$^{-1}$) (Goesmann et al., 2017) or a longer duration of the pyrolysis experiment could help the detection of diphenylmethane, triphenylmethane and phenyl fluorene released from the pyrolysis of benzoate salts.

### 4.3. Wet chemistry

Finally, when derivatized with DMF-DMA, MTBSTFA or TMAH, both the acid and the organic salt produced the same derivatized product. With MTBSTFA, the calcium salts derivatized better than their acid.

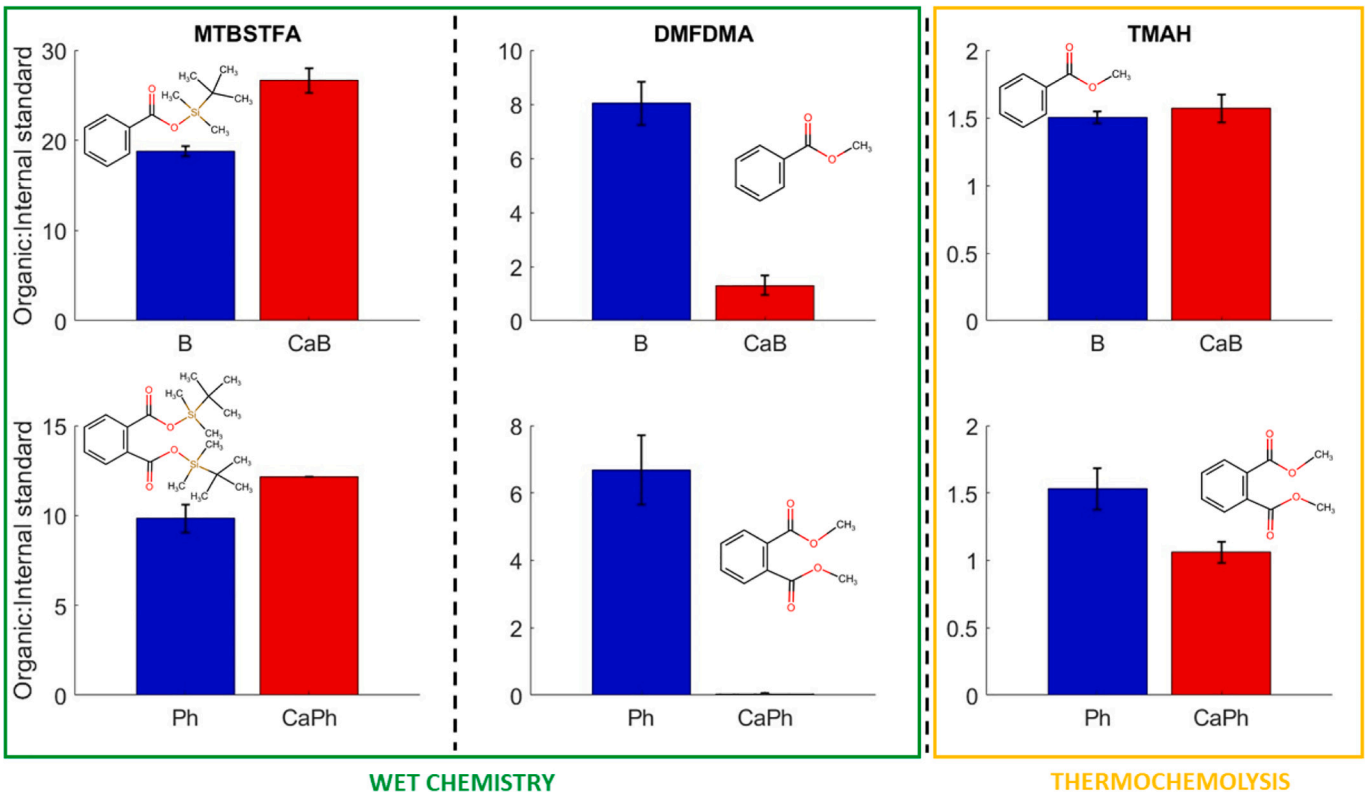


**Fig. 9.** Comparison of the derivatization and thermochemolysis efficiencies of MTBSTFA (left), DMF-DMA (middle) and TMAH (right) reagents as measured by the abundance of derivatized compound obtained with the salt and the acid form of benzoic acid and phthalic acid derivatized, relative to the naphthalene $d_8$ internal standard. Both acid/salt couple samples were equimolar. Benzoic acid (B), calcium benzoate (CaB), phthalic acid (Ph), calcium phthalate (CaPh). Wet chemistry and thermochemolysis yield are not to be compared as the protocols and instrument used are different.

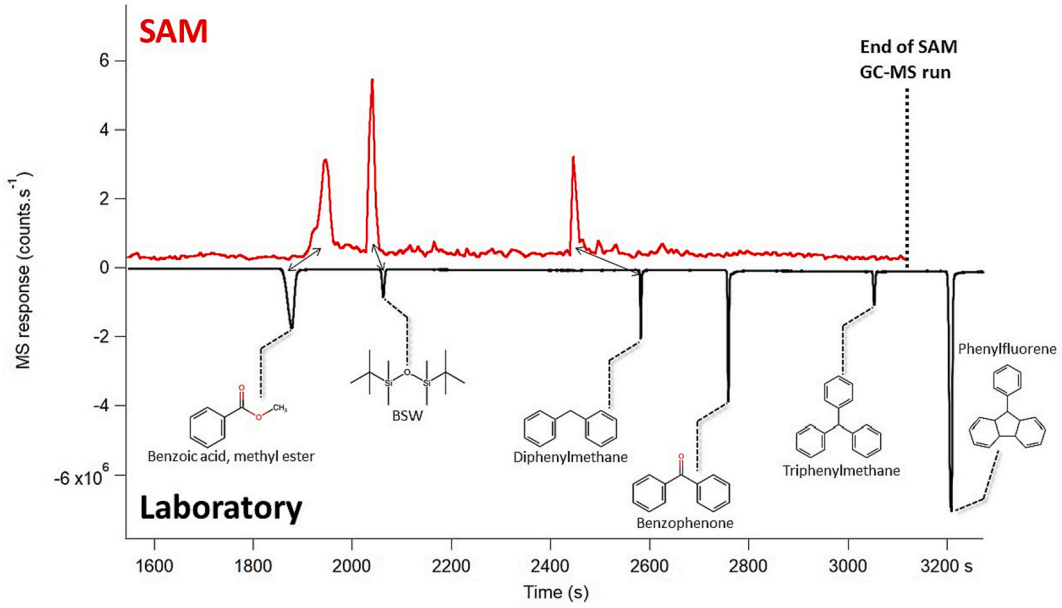


**Fig. 10.** GC–MS analyses of selected pyrolysis and derivatization products of organic salts in a laboratory GC-2 column (bottom) compared to the same species detected in a SAM chromatogram (top). The reconstructed SAM chromatogram is from the analysis of the Mary Anning sample where the mass to charge ratios ($m/z$) were adjusted as followed: m/z 105*60 + m/z 147 + m/z 167*600. The temperature program starts at T1 = 45 °C for 7 min, followed by a first ramp of 120 °C.min$^{-1}$ to T2 = 66 °C, then a second ramp od 0.3 °C.min$^{-1}$ to T3 = 59 °C and finally a third ramp of 10 °C.min$^{-1}$ to reach a final temperature of 280 °C for 30 min. The inlet column pressure was set to 130 kPa to match the retention time of the bi-silylated water (BSW) observed at 34.54 min on SAM.

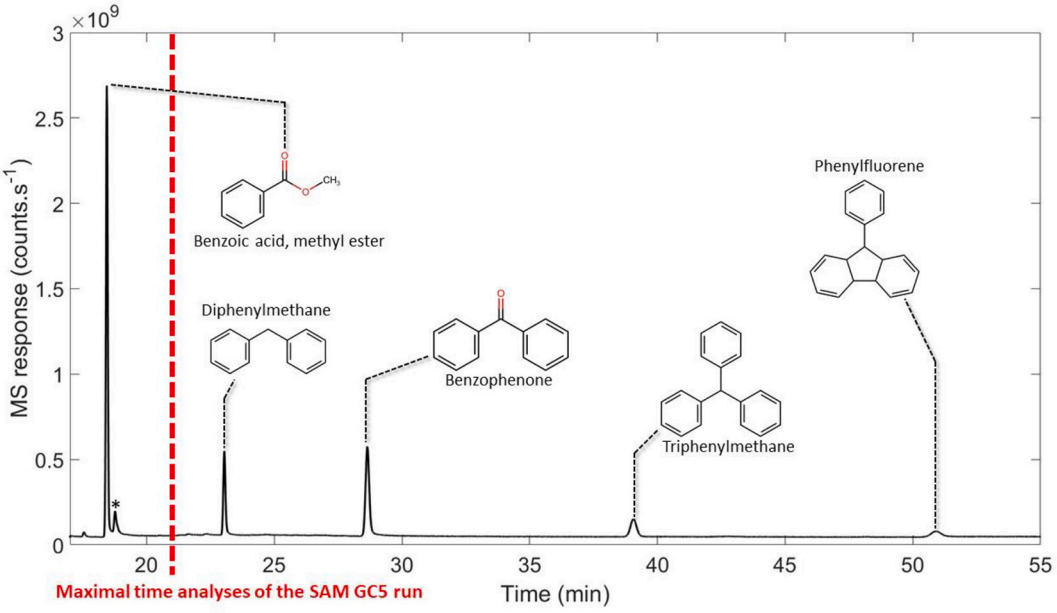


**Fig. 11.** Laboratory GC–MS analyses of the characteristic pyrolysis and derivatization products of organic salts in SAM GC5 conditions. The maximal time of analyses of the SAM GC5 run *in situ* is 21 min. (*) artifact of the column (stationary phase bleeding).

Whereas with DMF-DMA, a higher derivatization yield was observed for the acid than for the salt. Moreover, with TMAH, the benzoic acid and salt had a similar derivatization yield, whereas, phthalic acid derivatized better than its salt counterpart. Therefore, when derivatized with DMF-DMA or TMAH, calcium lowers the availability of the labile group during the derivatization process. The derivatization reagents can readily react with the labile hydrogen of the carboxylic group of the acid, whereas the salts are in their anionic form, decreasing the reactivity of the reagent toward the salt. The presence of the calcium cation also increased the steric hindrance of the molecules and therefore decreased the access of the derivatization reagent to the reactive group.

Moreover, when comparing the yield between the wet chemistry experiments, we obtained a higher relative abundance of derivatized molecules for both the acid and the salt with MTBSTFA compared to DMF-DMA. This could be explained by a difference in the mass spectrometer's response for DMF-DMA and MTBSTFA derivatized compounds. Molecule derivatized with MTBSTFA could be better ionized in the mass spectrometer source than compounds derivatized with DMF-DMA because the *tert*-butyldimethylsilyl group added by MTBSTFA has a higher ionization cross section compared to the methyl group added by DMF-DMA. Moreover, the derivatization response is higher for compounds derivatized with MTBSTFA than molecules derivatized with DMF-DMA. Combined, this could explain the highest detection of MTBSTFA derivatized compounds compared to those with DMF-DMA. These results showed that MTBSTFA would be better suited for the derivatization of these salts if present in the Martian soil since these molecules may not be detectable using DMF-DMA. Furthermore, Williams et al. (2021), reported the potential detection of benzoic acid methyl ester in the first TMAH sample of the SAM instrument suite and Millan et al. (2022) detected benzoic acid *tert*-butyldimethylsilyl in the Ogunquit Beach (OG) sample collected in the sand of Bagnold Dunes by the Curiosity rover. Therefore, if present in the Martian soil, aromatic calcium salts could be derivatized through wet chemistry or thermochemistry experiments present on SAM and MOMA, showing the complementarity of this technique with pyrolysis.

## 5. Conclusions and perspectives

These results showed that sample pyrolysis, can provide a signature of parent carboxylic acid molecules but not aromatic calcium salts where only byproducts were produced. If present at the Martian surface, aromatic carboxylic salts, such as calcium benzoate and phthalate, could be detected indirectly through high temperature (> 500 °C) thermal extraction analysis such as EGA or pyrolysis-GC–MS or wet chemistry experiments, showing that the missing organic molecules described by Benner et al. (2000) could be identified with instrumental set-ups such as SAM or MOMA. This shows the importance of using the different capabilities of these instrument suites in tandem to understand more deeply the data obtained from a sample and increase the possibility to detect refractory molecules. However, the low intensity of the compounds identified in the organic salt pyrolysis chromatogram could fall below the detection limit of the instruments. This observation also agrees with Benner et al.'s conclusion regarding the probable low capability of the Viking GC–MS instruments to detect certain organics such as salts of benzenecarboxylic acids.

Overall, the conclusions of this work raise essential questions on the detectability of refractory molecules and on the interpretation of *in situ* data. To expand this work, experimental study on the high-fidelity Engineering Test Unit (ETU) and/or testbeds of MOMA and SAM instrument suites could help further understand the signature and behavior of aromatic organic salts under relevant Mars operational conditions. Furthermore, matrices with relevant lithologies to the Martian surface should be used to study the reactivity of the aromatic organic salts during *in situ* measurements. Finally, this study focused only on calcium organic salts, other cations, likely to be present on Mars like iron or magnesium, should be tested in order to compare their influence on the thermal degradation and derivatization of the molecules.

## CRediT authorship contribution statement

**O. McIntosh:** Conceptualization, Data curation, Formal analysis, Investigation, Methodology, Validation, Visualization, Writing – original draft, Writing – review & editing. **C. Freissinet:** Conceptualization, Funding acquisition, Methodology, Project administration, Supervision, Validation, Writing – review & editing. **A. Buch:** Conceptualization, Supervision, Validation, Visualization, Writing – review & editing. **J.M. T. Lewis** Writing – review & editing. **M. Millan:** Writing – review & editing. **A.J. Williams:** Writing – review & editing. **T. Fornaro:** Writing

– review & editing. **J.L. Eigenbrode** Writing – review & editing. **J. Brucato:** Writing – review & editing. **C. Szopa:** Conceptualization, Funding acquisition, Project administration, Resources, Supervision, Validation, Visualization, Writing – review & editing.

## Declaration of competing interest

The authors declare that they have no known competing financial interests or personal relationships that could have appeared to influence the work reported in this paper.

## Data availability statement

Sam data can be accessed *via* the Planetary Data System http://pds-geosciences.wustl.edu/missions/msl/.

## Acknowledgments

The authors acknowledge the financial support the French national space agency, the Centre National d'Etudes Spatiales (CNES) (SAM-GC and MOMA-GC grants) and the "ADI 2020" project funded by the IDEX Paris-Saclay, ANR-11-IDEX-0003-02. We acknowledge the help of Fred Goesmann for his insightful support and inputs. The authors declare no conflicts of interest.

## References

Benner, S.A., Devine, K.G., Matveeva, L.N., Powell, D.H., 2000. The missing organic molecules on Mars. Proc. Natl. Acad. Sci. 97 (6), 2425–2430. https://doi.org/10.1073/pnas.040539497.

Brass, G.W., 1980. Stability of brines on Mars. Icarus 42 (1), 20–28.

Buch, A., Belmahdi, I., Szopa, C., Freissinet, C., Glavin, D.P., Millan, M., Summons, R., Coscia, D., Teinturier, S., Bonnet, J.Y., He, Y., Cabane, M., Navarro-Gonzalez, R., Malespin, C.A., Stern, J., Eigenbrode, J., Mahaffy, P.R., Johnson, S.S., 2019. Role of the Tenax® adsorbent in the interpretation of the EGA and GC-MS analyses performed with the sample analysis at Mars in Gale crater. J. Geophys. Res.: Planets 124 (11), 2819–2851. https://doi.org/10.1029/2019je005973.

Clark, B.C., Baird, A., Rose Jr., H.J., Toulmin III, P., Keil, K., Castro, A.J., Kelliher, W.C., Rowe, C.D., Evans, P.H., 1976. Inorganic analyses of Martian surface samples at the Viking landing sites. Science 194 (4271), 1283–1288.

Clark, J.V., Sutter, B., McAdam, A.C., Rampe, E.B., Archer, P.D., Ming, D.W., Navarro-Gonzalez, R., Mahaffy, P., Lapen, T.J., 2020. High-temperature HCl evolutions from mixtures of perchlorates and chlorides with water-bearing phases: implications for the SAM instrument in Gale crater, Mars. J. Geophys. Res.: Planets 125 (2). https://doi.org/10.1029/2019je006173.

Dabestani, R., Britt, P.F., Buchanan, A.C., 2005. Pyrolysis of aromatic carboxylic acid salts: does decarboxylation play a role in cross-linking reactions? Energy Fuel 19 (2), 365–373. https://doi.org/10.1021/ef0400722.

Eigenbrode, J.L., Summons, R.E., Steele, A., Freissinet, C., Millan, M., Navarro-González, R., Sutter, B., McAdam, A.C., Franz, H.B., Glavin, D.P., Archer, P.D., Mahaffy, P.R., Conrad, P.G., Hurowitz, J.A., Grotzinger, J.P., Gupta, S., Ming, D.W., Sumner, D.Y., Szopa, C., Malespin, C., Buch, A., Coll, P., 2018. Organic matter preserved in 3-billion-year-old mudstones at Gale crater. Mar. Sci. 360 (6393), 1096–1101. https://doi.org/10.1126/science.aas9185.

Fornaro, T., Steele, A., Brucato, J., 2018. Catalytic/protective properties of Martian minerals and implications for possible origin of life on Mars. Life 8 (4), 56. https://doi.org/10.3390/life8040056.

Fox, A.C., Eigenbrode, J.L., Freeman, K.H., 2019. Radiolysis of macromolecular organic material in Mars-relevant mineral matrices. J. Geophys. Res.: Planets 124 (12), 3257–3266. https://doi.org/10.1029/2019je006072.

Freissinet, C., Buch, A., Sternberg, R., Szopa, C., Geffroy-Rodier, C., Jelinek, C., Stambouli, M., 2010. Search for evidence of life in space: Analysis of enantiomeric organic molecules by N,N-dimethylformamide dimethylacetal derivative dependant Gas Chromatography–Mass Spectrometry. J. Chromatogr. A 1217 (5), 731–740. https://doi.org/10.1016/j.chroma.2009.11.009.

Freissinet, C., Glavin, D.P., Mahaffy, P.R., Miller, K.E., Eigenbrode, J.L., Summons, R.E., Brunner, A.E., Buch, A., Szopa, C., Archer, P.D., Franz, H.B., Atreya, S.K., Brinckerhoff, W.B., Cabane, M., Coll, P., Conrad, P.G., Des Marais, D.J., Dworkin, J. P., Fairén, A.G., François, P., Grotzinger, J.P., Kashyap, S., Ten Kate, I.L., Leshin, L. A., Malespin, C.A., Martin, M.G., Martin-Torres, F.J., McAdam, A.C., Ming, D.W., Navarro-González, R., Pavlov, A.A., Prats, B.D., Squyres, S.W., Steele, A., Stern, J.C., Sumner, D.Y., Sutter, B., Zorzano, M.P., 2015. Organic molecules in the Sheepbed mudstone, Gale crater, Mars. J. Geophys. Res.: Planets 120 (3), 495–514. https://doi.org/10.1002/2014je004737.

Freissinet, C., Knudson, C.A., Graham, H.V., Lewis, J.M., Lasue, J., McAdam, A.C., Teinturier, S., Szopa, C., Dehouck, E., Morris, R.V., 2020. Benzoic acid as the preferred precursor for the chlorobenzene detected on Mars: insights from the unique Cumberland analog investigation. Planet. Sci. J. 1 (2), 41.

Glavin, D.P., Freissinet, C., Miller, K.E., Eigenbrode, J.L., Brunner, A.E., Buch, A., Sutter, B., Archer, P.D., Atreya, S.K., Brinckerhoff, W.B., Cabane, M., Coll, P., Conrad, P.G., Coscia, D., Dworkin, J.P., Franz, H.B., Grotzinger, J.P., Leshin, L.A., Martin, M.G., McKay, C., Ming, D.W., Navarro-González, R., Pavlov, A., Steele, A., Summons, R.E., Szopa, C., Teinturier, S., Mahaffy, P.R., 2013. Evidence for perchlorates and the origin of chlorinated hydrocarbons detected by SAM at the Rocknest aeolian deposit in Gale crater. J. Geophys. Res.: Planets 118 (10), 1955–1973. https://doi.org/10.1002/jgre.20144.

Goesmann, F., Brinckerhoff, W.B., Raulin, F., Goetz, W., Danell, R.M., Getty, S.A., Siljeström, S., Mißbach, H., Steininger, H., Arevalo, R.D., Buch, A., Freissinet, C., Grubisic, A., Meierhenrich, U.J., Pinnick, V.T., Stalport, F., Szopa, C., Vago, J.L., Lindner, R., Schulte, M.D., Brucato, J.R., Glavin, D.P., Grand, N., Li, X., Van Amerom, F.H.W., Science, The Moma, T., 2017. The Mars organic molecule analyzer (MOMA) instrument: characterization of organic material in Martian sediments. Astrobiology 17 (6–7), 655–685. https://doi.org/10.1089/ast.2016.1551.

Hakkinen, S.A., McNeill, V.F., Riipinen, I., 2014. Effect of inorganic salts on the volatility of organic acids. Environ. Sci. Technol. 48 (23), 13718–13726. https://doi.org/10.1021/es5033103.

Hassler, D.M., Zeitlin, Cary, Robert, F., Schweingruber, Wimmer, Ehresmann, Bent, Rafkin, Scot, Eigenbrode, L.J., Brinza, David E., Weigle, Gerald, Böttcher, Stephan, Böhm, Eckart, Burmeister, Soenke, Guo, Jingnan, Köhler, Jan, Martin, Cesar, Reitz, Guenther, Cucinotta, Francis A., Myung-Hee, Kim, Grinspoon, David, Bullock Arik Posner, Mark A., Javier, Gómez-Elvira, Vasavada, Ashwin, Grotzinger, John P., MSL, & Team, S, 2013. Mars' surface radiation environment with the Mars Science Laboratory's curiosity rover. Science. https://doi.org/10.1126/science.1244797.

Jehlička, J., Edwards, H., 2008. Raman spectroscopy as a tool for the non-destructive identification of organic minerals in the geological record. Org. Geochem. 39 (4), 371–386.

Karunatillake, S., Keller, J.M., Squyres, S.W., Boynton, W.V., Brückner, J., Janes, D.M., Gasnault, O., Newsom, H.E., 2007. Chemical compositions at Mars landing sites subject to Mars odyssey gamma ray spectrometer constraints. J. Geophys. Res.: Planets 112 (E8). https://doi.org/10.1029/2006je002859.

Kminek, G., Bada, J.L., 2006. The effect of ionizing radiation on the preservation of amino acids on Mars. Earth Planet. Sci. Lett. 245 (1–2), 1–5.

Lasne, J., Noblet, A., Szopa, C., Navarro-Gonzalez, R., Cabane, M., Poch, O., Stalport, F., Francois, P., Atreya, S.K., Coll, P., 2016. Oxidants at the surface of Mars: a review in light of recent exploration results. Astrobiology 16 (12), 977–996. https://doi.org/10.1089/ast.2016.1502.

Lewis, J.M.T., Eigenbrode, J.L., Wong, G.M., McAdam, A.C., Archer, P.D., Sutter, B., Millan, M., Williams, R.H., Guzman, M., Das, A., Rampe, E.B., Achilles, C.N., Franz, H.B., Andrejkovičová, S., Knudson, C.A., Mahaffy, P.R., 2021. Pyrolysis of oxalate, Acetate, and Perchlorate Mixtures and the Implications for Organic Salts on Mars. J. Geophys. Res.: Planets 126 (4). https://doi.org/10.1029/2020je006803.

Mahaffy, P.R., Webster, C.R., Cabane, M., Conrad, P.G., Coll, P., Atreya, S.K., Arvey, R., Barciniak, M., Benna, M., Bleacher, L., Brinckerhoff, W.B., Eigenbrode, J.L., Carignan, D., Cascia, M., Chalmers, R.A., Dworkin, J.P., Errigo, T., Everson, P., Franz, H., Farley, R., Feng, S., Frazier, G., Freissinet, C., Glavin, D.P., Harpold, D.N., Hawk, D., Holmes, V., Johnson, C.S., Jones, A., Jordan, P., Kellogg, J., Lewis, J., Lyness, E., Malespin, C.A., Martin, D.K., Maurer, J., McAdam, A.C., McLennan, D., Nolan, T.J., Noriega, M., Pavlov, A.A., Prats, B., Raaen, E., Sheinman, O., Sheppard, D., Smith, J., Stern, J.C., Tan, F., Trainer, M., Ming, D.W., Morris, R.V., Jones, J., Gundersen, C., Steele, A., Wray, J., Botta, O., Leshin, L.A., Owen, T., Battel, S., Jakosky, B.M., Manning, H., Squyres, S., Navarro-González, R., McKay, C. P., Raulin, F., Sternberg, R., Buch, A., Sorensen, P., Kline-Schoder, R., Coscia, D., Szopa, C., Teinturier, S., Baffes, C., Feldman, J., Flesch, G., Forouhar, S., Garcia, R., Keymeulen, D., Woodward, S., Block, B.P., Arnett, K., Miller, R., Edmonson, C., Gorevan, S., Mumm, E., 2012. The sample analysis at Mars investigation and instrument suite. Space Sci. Rev. 170 (1–4), 401–478. https://doi.org/10.1007/s11214-012-9879-z.

Millan, M., Szopa, C., Buch, A., Coll, P., Glavin, D.P., Freissinet, C., Navarro-Gonzalez, R., François, P., Coscia, D., Bonnet, J.Y., Teinturier, S., Cabane, M., Mahaffy, P.R., 2016. In situ analysis of martian regolith with the SAM experiment during the first mars year of the MSL mission: identification of organic molecules by gas chromatography from laboratory measurements. Planet. Space Sci. 129, 88–102. https://doi.org/10.1016/j.pss.2016.06.007.

Millan, M., Szopa, C., Buch, A., Cabane, M., Teinturier, S., Mahaffy, P., Johnson, S., 2019. Performance of the SAM gas chromatographic columns under simulated flight operating conditions for the analysis of chlorohydrocarbons on Mars. J. Chromatogr. A 1598, 183–195.

Millan, M., Szopa, C., Buch, A., Summons, R.E., Navarro-Gonzalez, R., Mahaffy, P.R., Johnson, S.S., 2020. Influence of calcium perchlorate on organics under SAM-like pyrolysis conditions: constraints on the nature of Martian organics. J. Geophys. Res.: Planets 125 (7). https://doi.org/10.1029/2019je006359.

Millan, M., Teinturier, S., Malespin, C., Bonnet, J., Buch, A., Dworkin, J., Eigenbrode, J., Freissinet, C., Glavin, D., Navarro-González, R., 2022. Organic molecules revealed in Mars's Bagnold dunes by Curiosity's derivatization experiment. Nature Astronomy 6 (1), 129–140.

Ming, D.W., Archer Jr., P., Glavin, D., Eigenbrode, J., Franz, H., Sutter, B., Brunner, A., Stern, J., Freissinet, C., McAdam, A., 2014. Volatile and organic compositions of sedimentary rocks in Yellowknife Bay, Gale crater, Mars. Science 343 (6169), 1245267.

Nachon, M., Mangold, N., Forni, O., Kah, L., Cousin, A., Wiens, R., Anderson, R., Blaney, D., Blank, J., Calef, F., 2017. Chemistry of diagenetic features analyzed by ChemCam at Pahrump Hills, Gale crater, Mars. Icarus 281, 121–136.

Oró, J., Holzer, G., 1979a. The effects of ultraviolet light on the degradation of organic compounds: a possible explanation for the abscence of organic matter on Mars. Life Sci. Space Res. 77-86 https://doi.org/10.1016/b978-0-08-023416-8.50013-1.

Oró, J., Holzer, G., 1979b. The photolytic degradation and oxidation of organic compounds under simulated Martian conditions. J. Mol. Evol. 14 (1–3), 153–160. https://doi.org/10.1007/bf01732374.

Pavlov, A.A., McLain, H.L., Glavin, D.P., Roussel, A., Dwork2in, J. P., Elsila, J. E., & Yocum, K. M., 2022. Rapid Radiolytic degradation of amino acids in the Martian shallow subsurface: implications for the search for extinct life. Astrobiology 22 (9), 1099–1115.

Rampe, E.B., Blake, D.F., Bristow, T.F., Ming, D.W., Vaniman, D.T., Morris, R.V., Achilles, C.N., Chipera, S.J., Morrison, S.M., Tu, V.M., Yen, A.S., Castle, N., Downs, G.W., Downs, R.T., Grotzinger, J.P., Hazen, R.M., Treiman, A.H., Peretyazhko, T.S., Des Marais, D.J., Walroth, R.C., Craig, P.I., Crisp, J.A., Lafuente, B., Morookian, J.M., Sarrazin, P.C., Thorpe, M.T., Bridges, J.C., Edgar, L. A., Fedo, C.M., Freissinet, C., Gellert, R., Mahaffy, P.R., Newsom, H.E., Johnson, J.R., Kah, L.C., Siebach, K.L., Schieber, J., Sun, V.Z., Vasavada, A.R., Wellington, D., Wiens, R.C., 2020. Mineralogy and geochemistry of sedimentary rocks and eolian sediments in Gale crater, Mars: a review after six earth years of exploration with curiosity. Geochemistry 80 (2), 125605. https://doi.org/10.1016/j.chemer.2020.125605.

Rapin, W., Ehlmann, B.L., Dromart, G., Schieber, J., Thomas, N., Fischer, W.W., Fox, V., Stein, N.T., Nachon, M., Clark, B.C., 2019. An interval of high salinity in ancient Gale crater lake on Mars. Nat. Geosci. 12 (11), 889–895.

Schlten, H.-R., Leinweber, P., 1993. Pyrolysis-field ionization mass spectrometry of agricultural soils and humic substances: effect of cropping systems and influence of the mineral matrix. Plant Soil 151, 77–90.

Seelos, K.D., Seelos, F.P., Viviano-Beck, C.E., Murchie, S.L., Arvidson, R.E., Ehlmann, B. L., Fraeman, A.A., 2014. Mineralogy of the MSL curiosity landing site in Gale crater as observed by MRO/CRISM. Geophys. Res. Lett. 41 (14), 4880–4887. https://doi.org/10.1002/2014gl060310.

Szopa, C., Freissinet, C., Glavin, D.P., Millan, M., Buch, A., Franz, H.B., Summons, R.E., Sumner, D.Y., Sutter, B., Eigenbrode, J.L., Williams, R.H., Navarro-González, R., Guzman, M., Malespin, C., Teinturier, S., Mahaffy, P.R., Cabane, M., 2020. First detections of dichlorobenzene isomers and Trichloromethylpropane from organic matter indigenous to Mars mudstone in Gale crater, Mars: results from the sample analysis at Mars instrument onboard the curiosity rover. Astrobiology 20 (2), 292–306. https://doi.org/10.1089/ast.2018.1908.

Toulmin III, P., Clark, B.C., Baird, A., Keil, K., Rose Jr., H.J., 1976. Preliminary results from the Viking X-ray fluorescence experiment: the first sample from Chryse Planitia. Mar. Sci. 194 (4260), 81–84.

Williams, A., Eigenbrode, J., Millan, M., Williams, R., Buch, A., Teinturier, S., Glavin, D., Freissinet, C., Szopa, C., McIntosh, O., 2021. Organic molecules detected with the first TMAH wet chemistry experiment, Gale crater, Mars. 52nd lunar and planetary Science conference.